International Journal Of Earth Sciences
April 2020, Volume 109 Issue 3 Pages 847-876
https://doi.org/10.1007/s00531-020-01833-9
https://archimer.ifremer.fr/doc/00613/72489/

Volcanoes and climate: the triggering of preboreal Jökulhlaups in Iceland

Van Vliet-Lanoë Brigitte [1, *] , Knudsen Oskar [2], Guðmundsson Agust [3], Guillou Hervé [4], Chazot Gilles [1], Langlade Jessica [5], Liorzou Celine [1], Nonnotte Philippe [1]

[1] Géosciences Ocean, UMR 6538 Brest University, CNRS, ue@b, IUEM, Pl.N.Copernic, 29280, Plouzané, France
[2] Klettur Consulting Engineers, Bildshofda 12, 102, Reykjavik, Iceland
[3] Jarðfræðistofan ehf, 200, Hafnarfjorður, Iceland
[4] CNRS-CEA, UMR 8212 LSCE, Domaines CNRS, Bât. 12, Av. de la terrasse, 91198, Gif/Yvette, France
[5] Microsonde de l'Ouest, Ifremer-Centre de BretagneTechnopole Brest Iroise, BP 70, 29280, Plouzané, France

* Corresponding author : Brigitte Van Vliet-Lanoë, email address : brigitte.vanvlietlanoe@univ-brest.fr

Abstract :

The Early Holocene (12–8.2 cal ka) deglaciation and pulsed warming was associated in Iceland with two major generations of jökulhlaups around the Vatna ice-cap (Vatnajökull), at ca 11.4–11.2 cal ka and ca 10.4–9.9 cal ka, and major tephra emissions from the Grímsvötn and Bárðarbunga subglacial volcanoes. The earliest flood events were recorded inland during the Middle Younger Dryas and their deposits were overlain by the Early Preboreal Vedde Ash (11.8 cal ka). The first Holocene flood events (ca 11.4–11.2 cal ka) are issued from a glacial advance. The second, and major, set of floods was partly driven by the Erdalen cold events and advances (10.1–9.7 10Be ka) initially issued from the Bárðarbunga (10.4, 10.1–9.9 ka) and Grímsvötn volcanoes (Saksunarvatn tephra complex, ca. 10.2–9.9 cal ka). These floods were also fed by the residual glacio-isostatic depressions below the Vatnajökull that enabled the storage of meltwaters in large subglacial lakes or aquifers until ca. 9.3 cal ka. This storage was enhanced by ice-damming and permafrost, especially during the twinned Erdalen events. Due to the glacio-isostatic rebound, the general slope was nearly flat, and the valley was partly filled with sediments until ca 10.8 cal ka. Temporary lacustrine deposits in this valley resulted from the very broad splay of waters as for the ca 11.2 cal ka and ca 10.1–9.9 cal ka flood, due to regional permafrost. These floods had a potential duration of several months as they were mostly fed by climate-driven meltwater. The maximal volume evacuated by these events did not greatly exceed 1 × 106 m3 s−1 from the flood-affected transverse profile of the valleys that remain partly filled with sediments.

Keywords : Holocene, Deglaciation, Iceland, Geomorphology, Glacial, Flood, Sedimentology, Tephra, Glacio-isostatic rebound, Permafrost, Saksunarvatn event, Askja S

1. Introduction

Large-scale outburst flows were a common phenomenon that accompanied the termination of the last glaciation in non-volcanic regions (e.g. Carling 2013). Meltwater storage in or at the surface of a glacier favours jökulhlaup occurrence (Rushmer 2006; Carrivick et al. 2009). Jökulhlaups may be also triggered by volcanism. As volcanism and melting are enhanced by deglaciation (Jull and McKenzie, 1996; Slater et al. 1998; MacLennan et al. 2002; Sinton et al. 2005), these events are suspected having promoted both jökulhlaups and more explosive volcanism (Höskuldsson et al. 2006; Van Vliet-Lanoë et al. 2007; Carrivick et al. 2009).

The analysis of the Early Holocene (ICS 2018) deglaciation in Iceland is a favourable place to understand their interrelations due to the radial organization of the drainage around the Vatnajökull (Fig. 1), the largest Late Holocene ice-cap.

Major active volcanic systems, with an extensive morphological impact, exist beneath the Vatnajökull (Fig. 1B) in the form of the Grímsvötn and Bárðarbunga Volcanoes (Björnsson 2017). The Vatnajökull rests on porous volcanogenic sediments on the western side of the Grímsvötn caldera, and on the impermeable bedrock below the Brúarjökull glacier and to the east (Flowers et al. 2003). Subglacial eruptions, associated with tephra outfalls from the Grímsvötn calderas, were responsible for numerous hazardous jökulhlaups to the north and south (Thorarinsson 1974; Björnsson 1992; Thordarson and Larsen 2007). The relationship between jökulhlaups and the last deglaciation is not analysed in Iceland, even though most of the terminal moraines in the south have been carefully described by Kaldal and Víkingsson (1990) and a chronology of jökulhaup events has been extracted from the lacustrine record of the deglaciation by Geirsdóttir et al. (2000).

The interval analysed in this paper covers the Younger Dryas to the Holocene Thermal Optimum (12.8 - 8 cal ka). The period from Termination Ib (11.8 cal ka, ICS 2018) to the Thermal Optimum (8–6 cal ka) was characterised in the south of Iceland (Fig. 1a) by a series of jökulhlaups (Geirsdóttir et al. 2000). In the southernmost Iceland, the first major Early Holocene eruption after Termination Ib and the deposition of the Vedde Ash was the Saksunarvatn Tephra (Mangerud et al. 1986). This was issued from the Grímsvötn Volcano at ca. 10.28 cal ka BP (Tephrabase), and was a potential trigger of major jökulhlaups. This volcano generated a large jökulhlaup via the Skeiðarárjökull Glacier (Fig.1B),

which delivered turbidites to the Mýrdalsjökull Submarine Canyon at ca 10.15 cal ka (Fig.1B, Lacasse et al. 1998). The source of the largest Holocene jökulhlaup events in the north is commonly attributed to the Grímsvötn and Kverkfjöll calderas (Sæmundsson 1973; Carrivick 2007; Carrivick et al. 2009) with another source in the Bárðarbunga subglacial caldera (Björnsson and Einarsson 1991; Waitt 2002; Fig. 1A, 2, 3A). These volcanoes were also responsible for jökulhlaups during the Eemian and the Holocene in the south, e.g. along the Jökulsá á Fjöllum and Þjorsá–Ytrí Rangá Rivers (Van Vliet-Lanoë et al. 2018).

In the North, most studies up to now have been focused on the main channel of the Jökulsá á Fjöllum (Fig.1a) and its morphologies (e.g. Middle Holocene floods: Kirkbride et al. 2006; synthesis in Baynes et al. 2015), but little attention has been paid to traces existing outside the canyon, especially on the nearby plateau, or upstream of adjacent dry valleys. This valley experienced multiple jökulhlaups of varying sizes following Termination Ib, as evidenced by a sequence of prehistoric flood deposits in the river canyon (e.g. Björnsson and Kristmannsdóttir, 1984) and on the upper terraces (this paper).

In this paper, we attempt to synthesize the existing published data, complemented with new observations that constrain the timing of the Holocene deglaciation and the early jökulhlaup events. It will be related to the Preboreal glacial advances and retreats, and their respective dynamic conditions. We first searched for key sedimentary sections with available chronological markers constraining intime as tephra the deglaciation history inland and on the continental shelf. The gathered data, including the permafrost information, was correlated with the climatic framework of the Early Holocene. Following this, we have tried to constrain the impact of the Early Holocene deglaciation on the Vatnajökull hydrological system and jökulhlaup recurrences. Control of glacio-isostasy and its impact on the volcanism was analysed, with a special focus on the complex Saksunarvatn tephra.

2. Methodology

Most of this work was performed on digital satellite images and aerial photos black and white and colour provided mostly by Landmælingar Íslands (National Land Survey of Iceland) and occasionally Google Earth (GE) for various dates, complemented by the photographic interpretations of Kaldal and Vikingsson (1990), Sæmundsson et al. (2012) and Sigurgeirsson et al. (2015). In terms of glaciation,

attention was primarily paid to fluted morphologies, “pitted” or hummocky moraines, surge moraines and normal terminal moraines (Fig. 1B), in an attempt to place them within a chronological framework. The development of specific periglacial morphologies (pattern grounds, rock glaciers) was used to delimit the glacier boundaries (Guðmundsson 2000). Erosional and sedimentary morphologies induced by flood activities (e.g. Maizel 2009; Baynes et al. 2015) were analysed using the same images as for the glacial morphology: channeled scablands with scourings, canyons and plunge basins, dry perched valleys, dismantled surfaces of lava flows, potholes, pillars and rough surfaces on consolidated sediments, streamlined residual landforms, fluviatile dunes. These morphologies were used to map the maximal flood extent (Fig. 1A).

The tephra record used herein (Table 1) refers to the published data from Icelandic lakes and soils, and the marine- and ice-core records (Greenland and Iceland shelf; Wohlfarth et al. 2006; Koren et al. 2008; Lind and Wastegård 2011; Óladóttir et al. 2011; Larsen et al. 2012; Voelker and Haflidason 2015; Guðmundsdóttir et al. 2016). Tephra and sediments were analysed in bulk by ICP–MS AES to determine their sources, with single-grain microprobe and laser ICP–MS being used to determine the source of rhyolitic tephra. Tephra-derived ages are given in c. X cal ka (BP), to avoid repetition of error margins, most of them being established on age models.

3. Paleoclimate and volcanic context

3.1. Deglaciation context and climate

The onset of the Younger Dryas (YD, 12.9 cal ka) was driven both by Oceanic circulation perturbation (Condron and Winsor 2012) and by a major solar minimum (Andresen et al. 2000; Goslar et al 2000). Since the YD, the Northern Hemisphere deglaciation has proceeded with brief, discrete cooling events, at c. 11.3–11.1 cal ka , 10.3, 9.3 and 8.2 cal ka (Fig.3), associated with the advance of glaciers (North Greenland Ice Core Project [NGRIP], 2004). Four episodes of glacier advance fit the cooling events thatbeen recognised in the ocean (Bond et al. 2001), in Scandinavia, the Færoe Islands and Greenland (Rasmussen et al. 2006; Matthews et al. 2008; Geirsdóttir et al. 2009; Kobashi et al. 2017): the Preboreal oscillation (11.3–11.1 cal ka; the 10.3-10.2 cal ka / 10.1-9.7 ^{10}Be ka cooling or Erdalen cooling events (Fig.3) allegedly driven by volcanic activity (Linde and Wastergård, 2011; Rasmussen et al. 2014) and a c. 9.3 cal ka cooling linked to a solar low that lasted for over 50 years (^{10}Be; Björck

et al. 1997; Bos et al. 2007). The youngest, the classical “8.2 cal ka” cooling event was the longest and coolest lasting for the next two to four centuries (Matero et al. 2017). This cooling seems triggered by solar activity (Stuiver and Braziunas 1988; Bond et al. 2001; Vonmoos et al. 2006), by a major meltwater pulse, issued from the Laurentide Ice Sheet collapse (Matero et al. 2017) with some impact of volcanic activity (Kobashi et al. 2017).

The Early Holocene pulsed warming was associated with the restoration of the North Atlantic and Irminger Currents, which increased the temperature and precipitation resulting in an accelerated ice-sheet retreat in Iceland (Jennings et al. 2000). The main Icelandic ice-sheet retreated rapidly across the highlands at that time (Geirsdóttir et al. 2009). After the “8.2 cal ka” cooling, the glaciers almost disappeared in Iceland. The thermal optimum was apparently ca. 2°C – 3°C higher than today (Andresen et al. 2007; Geirsdóttir et al. 2009; Langdon et al. 2010).

The Younger Dryas cooling has a duration of 1 ka (Condron and Winsor 2012), long enough for promoting glacier advances as demonstrated for the North by the ^{36}Cl dating of rockglaciers and coastal deposits (Andrès et al. 2016; Andrès et al. 2019), but not for restoring the ice-sheet, as has been commonly proposed (Norðdhal and Petursson, 2005; Patton et al. 2015) on the base of radiocarbon dated coastal deposits. This restricted extent is demonstrated in the west of the island by the limited glacioisosatic rebound of the YD (Brader et al. 2015). The YD seems to have been associated with the spreading of ice-lobes in the south (Geirsdóttir et al. 2009; Van Vliet-Lanoë et al. 2018) although the tidal glacier or ice-streams, calving into the coastal bays, occupied the valleys in the west and the north (Fig. 1; Jennings et al. 2007; Geirsdóttir et al. 2009; Andrès et al. 2019).

The durations of the pulsed Holocene cooling events were relatively short, with ca 150 years for the “10.3 cal ka“ twinned events, 50 to 200 years for the “9.3 cal ka” event and 200 to 400 years for the “8.2 cal ka” event (Rasmussen et al. 2006; Matero et al. 2017). They are considered to have been insufficient to have favoured ice-sheet development or major valley glacier advances during the Holocene. However, they were sufficient enough to have promoted glacier surges (Meier and Post, 1969).

3.2 Glaciers and permafrost

3.3 Subglacial volcanoes

The Grímsvötn volcanic system is believed to have been the most active volcano during the Holocene (Björnsson 1974; Larsen et al. 1998; Óladóttir et al. 2011), with an eruption frequency quite constant through time, and higher activity cycles, 60 to 80 years long. This volcano appears to have two reservoirs – a deeper one at 15 km depth and a shallow one at 3 km depth (Reverso et al. 2014) probably very reactive to deglaciation events via unloading (Hoskuldsson et al. 2006). Its large calderas, 3.6 km^3 in volume, is a major zone of meltwater storage, and a source for jökulhlaups, especially along the southern coast (Björnsson 2002). The detailed geochemistry of the Grímsvötn eruptions (single-grain laser ICP–MS) is not suitable for dating, as very few variations were recorded during the Holocene (Oladóttir et al. 2014; Thordarson 2014).

The Bárðarbunga Volcano, located at the NW edge of Vatnajökull, forms a wide and elevated caldera (1850 masl), completely glacier covered and is located along the extensive Veiðivötn fissure system, which parallels the Grímsvötn fissure system. The reservoir is located at a depth of 12 km (Guðmundsson et al. 2016). During the Holocene, the eruption frequency was five eruptions per century (Óladóttir et al. 2011). Its wide caldera, 14.4 km^3 in volume, has been a major source for jökulhlaups, especially in the southern embayment (Björnsson 2002). The Bárðarbunga Volcano had probably already been emerging from the ice-sheet since Bölling times, based on the tephra record (Table 1), producing five significant eruptions, at c.11.35, 11 – 10.8, 10.4, 10.1 and 9.9 cal ka (Óladóttir et al. 2011). .

3.4. The Askja rhyolitic tephra

Questions exist in the literature concerning the Askja 10/S Tephra, first described in Iceland and observed in Eyafjördur above the Vedde Ash (Sigurðsson and Sparks 1978; Askja 10) and below the Reitsvik 8 Tephra (c.10.2 cal ka; Larsen et al. 2002; Guðmundstottir et al. 2016). The classic Askja S Tephra age is now 10.8 cal ka (Wolfarth et al. 2006; Bronk et al. 2015; Table 1). In the Early Holocene, the Askja Volcano emitted probably at least five rhyolitic tephra, at c. 9.4 cal ka, c. 10.4 cal ka (10.5 – 10.35 cal ka; Lind and Wastegård 2011), 10.8 cal ka (Askja S), c. 11.5 cal ka (Ott et al. 2016), and c. 12.5 and 12.9 cal ka (Jones et al. 2017). The Kraþla 10 Tephra (Sæmundsson et al. 2012), very likely equates to the Reitsvík 8 Tephra (10.2 cal ka; Guðmundsdóttir et al. 2016), based on the available geochemical analysis (Krafla Phase 3; Jonásson 1994) but is hard to distinguish.

197

198 *3.5 The Saksunarvatn basaltic tephra*

199 The most common and thick tephra during the deglaciation is the Saksunarvatn Tephra (ca. 10.3 cal
200 ka; Mangerud et al. 1986; Fig.3). Dates for this very large deposit (> 15 km^3) cover several eruptive
201 events. In the Icelandic lake cores, there are up to six Early Holocene tephra layers with a Grímsvötn
202 chemical composition (Jóhannsdóttir, 2007; Fig.2A). The Saksunarvatn Tephra has not been recorded
203 in the Jökulsà à Fjöllum, although it is present in the Eyafjördur Fjord (Fig.1A; Larsen and Eiríksson,
204 2007) and on the northern shelf (Eiríksson et al. 2000). In Iceland and Norway (Guðmundsdóttir et al.
205 2016; Andresen et al. 2007; Birks et al. 1996; Grönvold et al. 1995; Fig 1a), Saksunarvatn/Grímsvötn-
206 type ash sedimentation began at c. 10.24 cal ka and continued up to 9.9 cal ka. In marine cores, four
207 aerial Grímsvötn eruptions were recorded from 10.30 to 9.85 cal ka (marine age-model; Lacasse et al.
208 1998; Guðmundsdóttir et al. 2012; Voelker and Haflidason 2015). In Greenland ice cores, the ranges
209 are from 10.24 - 10.12 ka ice-core ka (Rasmussen et al. 2006). It thus seems that the major Grímsvötn
210 eruption took place at ca 10.24 cal ka, followed by serial eruptions until 10.12 cal ka. The Mýrdal
211 Canyon turbidite, identified in the south (10.15 cal ka) possibly corresponded to a large subglacial
212 flood.

213

214 *3.6 Holocene and historical jökulhlaups*

215 The Jökulsá á Fjöllum River is incised by many dry channels issued from jökulhlaups, mapped by
216 Sæmundsson et al. 2012). Most of the studies were conducted along the canyon. From 1600 until
217 1934 AD, one large jökulhlaup per decade was issued from the Grímsvötn volcanic system into the
218 Jökulsá á Fjöllum River (Björnsson and Kristmannsdóttir 1984), fitting more or less with the basic
219 decennial frequency of eruptions (Óladóttir et al. 2011). Some Holocene events have been detected in
220 the same river between 7.10 and 2.0 cal ka (Sæmundsson 1973; Tómasson 1973; Elíasson 1977;
221 Waitt 2002; Kirkbride et al. 2006; Baynes et al. 2015), and specifically at c.. 4.6 cal ka, 3 cal ka and 2
222 cal ka.

223 In the SW, the main jökulhlaup activities have been assigned to 12.0 – 11.2 cal ka and c. 10.3 – 9.9
224 cal ka, essentially from Hestvatn Lake stratigraphy (Geirsdóttir et al. 2000). In the east of this sector
225 (Þjórsá–Tungnaá river system), we have previously shown that, from 155 to 8 ka, most of the
226 jökulhlaups were issued from both the volcanoes (Van Vliet-Lanoë et al. 2018).

Historical jökulhlaups have also been analysed near the southern edge of the Vatnajökull, particularly in relation to the Skeiðarárjökull Glacier (southern Vatnajökull; Maizels, 1991, 1997; Snorrasson et al. 1997; Russell et al. 2001).

4. Results

4.1. Tephrostratigraphy

Tephrostratigraphy and geochemistry were used to clarify regionally the age attributions of different events observed on aerial photography and controlled in the field. All the geochemical data are shown in Table 2.

Askja S is the most frequently recorded tephra of the observed series (see also Supplement, Figs. 3, 4).The observed Askja S Tephra seems to be a mixture of rhyolitic and dacitic lavas, whilst the Askja E rhyolite is mixed with basaltic components that were issued from the Askja/Bárðarbunga and Torfa Volcanoes (Supplement Table 2).

We proposed the following nomenclature to simplify the reading in time of the observed tephra: the Askja E tephra, at ca 10.4 cal ka and the Askja S, corresponding to the classical ca 10.8 cal ka tephra, both predate the Erdalen Event; the Vedde Ash (11,8 cal ka) and the Askja PB tephra at ca 11.5 cal ka predate most of the Preboreal events; the Askja YD tephra at ca 12.5 and 12.9 cal ka related to the YD events were not observed in sections in the 4 investigated Vatnajökull outlets systems.

4.2 The Jökulsá á Fjöllum system *(Fig.2B)*

The Röndin coastal section records the whole Late Glacial, followed by the transgression of the Termination Ib (from radiocarbon analysis; Norðdhal and Pétursson, 2005). These deposits lap onto local Eemian deposits (Van Vliet-Lanoë et al. 2005). The canyon of the Jökulsá á Fjöllum River (Supplement Fig. 2) seems to be ancient (Sæmundsson, 1973; Wait, 2002) and was filled with ca. 100 m of lithified glaciofluvial and lacustrine sediments, overlaid by Saalian and Eemian deposits, forming a progradation in a pre-existing incision. These Eemian deposits crop out at several places in the valley Van Vliet-Lanoë et al. 2001, 2005; Fig. 2B- yellow stars; Supplement Fig. 2).

4.2.1 Left bank – Asbyrgi, Vestudalur and Hnausar

This sector has been classically analysed along the canyon from a morphological point of view (see § 3.6). Near the Asbyrgi dead-end, commonly attributed to prehistorical events, on the left bank, large flood evidence exists outside the canyon, in the form of vegetated fluviatile megaripple fields (west of the Klappir terrace; Fig. 4), at 170 and 202 masl, with a train of smaller megaripples (east of Lambafell; Fig. 4).

In continuation of Asbyrgi / Klappir main terrace, the Vesturdalur one and the canyon are occupied by the Hljóðaklettar sublacustrine rootless basalt injections (Vesturdalur site, left bank; Hjartardóttir and Einarsson, 2017) estimated to be c. 10.8 ka in age, based on the Askja S Tephra analyses (Sigurgeirsson, 2016). They form a lava lake on the rocky valley bottom, close to the present river level, at an altitude of 145 – 150 masl (Fig. 2B; Supplement Fig. 3). The terrace on the left bank is topped at a 191 masl altitude by ca. 5 m of black tephra deposits and rootless cones with an Askja/Bárðarbunga geochemical signature (Table 2, sample Vest D2, see Supplement for pictures). This tephra being older than the overlying Askja E Tephra (10.4 cal ka; Table 2: Vest D3; Supplement Fig.3), seems to be local (lapilli from the rootless cones) but also associated with the Askja S Tephra (10.8 cal ka). On the other side of the valley, the fissural eruption feeding the Hljóðaklettar system consists of aerial cinder cones on the highest terrace, at 325 –350 masl, partly eroded by jökulhlaups. It issued from the Askja Volcanic system, and is subsynchronous with the Askja S Tephra (10.8 cal ka; Sigurgeirsson, 2016).

At the Hnausar site (Figs 2b-c, 4), 5 km south of Vestudalur site, new observations in quarries and roadworks have revealed jökulhlaup deposits perched high, at 392 masl, in a juxtaglacial position (kame terrace at 396 masl. These deposits are covered by three tephra in loesses: a Barðabunga basaltic tephra, a rhyolitic Vedde Ash (c. 11.8 cal ka) (Table 2), and a thin Askja tephra, probably PB (c. 11.5 ka; Table 2; Fig. 5B; Supplement Fig. 3E), These tephra are locally reworked by slack water deposits, and finally buried by grey and orange loesses, latterly reworked by a thin loessic stacked moraine (Fig. 5B). Down to Hólmatungur, these deposits are remolded by a large series of palaeolacustrine beaches attesting to an ephemeral palaeolake (Van Vliet-Lanoë et al. 2005) between 380 and 200 masl down to the Vestudalur terrace (Figs. 4, 5A). Two kilometers upstream of Hnausar, a complex morainic arc, at 390 masl, has been pierced by a flood along the Sauðadalur (Fig. 4 -5D).

Further upstream, an esker that issued from Lake Eilífisvötn (Fig. 4) joins the valley at Norðurfjöll,10 km further south, at ca. 400 masl, and has been partly eroded by flood waters below 380 masl.

On the right-bank, in front of Vesturdalur, the Hólssandur site (Kvensöðull) forms a wide terrace above the jökulsá canyon (Fig. 4). New observations have revealed highly visible asymmetrical-triangle-shaped remains of a morainic arc (Fig. 6C) that have been strongly eroded by floods. These relicts correspond to the Hnausar terminal moraine (Figs. 1B, 4). A fresh and broad splay of fine basaltic sand (Fig. 6A, B) was deposited at 2 km to the north, as a field of large fluviatile dunes, up to 380 masl and about 220 m above the present-day river (at 160 masl). These dunes lap onto intact orange loesses that contain a rhyolitic tephra, the Askja E (10.4 cal ka) and are surrounded by a dismantled lava flow from the c.10.8 cal ka Askja dyke, the cones of which have been abraded by jökulhlaups to c. 280 masl. The dune splay was formed on two successives phases, one subhorizontally laminated, the second incising and reworking the first deposit with megaripples. The end of alluvial sedimentation is recorded in impounded levels at the southern ends of the deposits. These deposits argue for a very limited slope at the time of the floods, and a flood trajectory located to the east of the canyon.

4.2.2 Hrossaborg tuff ring (close to the road N1)

The Hrossaborg tuff ring (Fig. 2B) is located in a graben in the middle of a valley. It consists of a phreatomagmatic cone, truncated and abraded by jökulhlaups (Alho, 2003), resting on a terrace, at 380 masl. One kilometer upstream, and to the west of the Hrossaborg crater, we observed the well visible asymmetrical-triangle-shaped 10 m high remains (Fig. 7A) of a morainic arc that has been strongly eroded by jökulhlaups. It is probably one of the traces within the valley axe of a younger advance compared to Hnausar, between Dettifoss and the Heirðubreid (Fig.2B).

4.2.3 Uppermost valley of the Jökulsá á Fjöllum (10 km north of the Vatnajökull)

In the uppermost valley of the Jökulsá á Fjöllum, the Vaðalda Volcano is sparsely splayed on its west flank by fresh basaltic tephra, to a limited altitude, 200 m above the Dyngjuvatn Lake surface. Field and image observations have revealed that fresh tephra fills the lake that occupies the crater depression (Fig. 7D). An associated train of large, flat slackwater dunes, subhorizontally laminated and now consolidated (25 m wide, 50 cm high; Fig. 7D), covers the Dyngjuvatn palaeolake surface up

317 to 688 masl. This deposit seems related to the rapid drainage of a larger lake, 'dammed' between the
318 Askja caldera and Vaðalda Volcano. The lake was issued from the Dyngjujökull Glacier (Fig. 1). The
319 dark, fine basaltic sand splay extends to the north, through Vikursandur, to the foot of the
320 Heiðubreiðartögl tuya, ending 1 km north of the confluence of the Jökulsá and Kreppa Rivers. It
321 reappears downstream, where it continues forming discrete terraces. These are higher in the
322 topography than the jökulhlaup features formerly described which splayed closer to the present course
323 of the Jökulsa River (Alho 2003, Alho et al. 2005; Carrivick et al.2013),.
324 The Kreppa River runs from the Brúarjökull outlet glacier (Fig. 2B), via the Kverká River, to the
325 extension of a major and incised subglacial plain (Björnsson, 2009). Downstream, in front of the
326 Heirðubreið Tuya, a dead valley diverges from the Kreppa River to the East, piercing a subglacial
327 volcanic ridge, and producing a giant, fresh basaltic crevasse splay with megaripples (20 m wide). This
328 abandoned channel is now drained by the Arnardalsá River, at 3 km to the North of a relatively fresh,
329 thin terminal moraine (Fig. 7B), which was issued erratically, straight from the Brúarjökull Glacier and
330 draining it. This moraine is only present on the eastern side of the Arnardalsalda hill, where it covers
331 the trace of an ancient braided channel. It was pierced by a jökulhlaup and further incised by
332 retrogressive scablands (Supplement Fig.1). .
333
334 *4.2.4 Synthesis for the Jökulsá á Fjöllum valley*
335 *Advances and deglaciation*
336 The Bölling deglaciation occurred quite far inland, south of the Þeistareykir Volcano (Figs 1, 3), prior to
337 10.8 cal ka (Askja S Tephra; Sæmundsson, 1992, 2002; Sigurgeirsson, 2016). This means that the YD
338 glaciers occupied the valleys, as shown by the presence of the Vedde Ash in a juxtaglacial position at
339 Hnausar (Fig. 5B), but the plateaus were only locally occupied by isolated ice-domes. The
340 tephrostatigraphy justifies an early deglaciation for the surge moraine, morainic arc and formation of
341 the Hnausar palaeolake, followed by the injection of the Hljóðaklettar rootless eruption (Figs 5, 6)
342 estimated at c. 11 – 10.8 cal ka (Sæmundsson et al. 2012; Sigurgeirsson, 2016) issued from the Askja
343 fissure system. The position of the main Preboreal moraine (ca 11.2 cal ka) was thus immediately
344 south of Hólssandur and at Hnausar.
345 The morainic arc preserved upstream close to the Hrossaborg is necessarily younger than Hnausar,
346 and it possibly corresponds to a glacial advance at ca 10.3 cal ka. This is henceforth called the

Hrossaborg Advance. The upstream of Morðrudalur, the single morainic arc issued straight from the Brúarjökull outlet glacier, despite the hilly morphology, remains untouched by large jökulhlaups (Fig.7B), excepted to the West. This advance is older than the Little Ice Age and potentially corresponds to the "9.3 cal ka" advance. The traces of this advance – probably a sudden surge – in the upper valley, are hereafter called the Kreppa Advance.

Jökulhlaups

Some early jökulhlaups occurred before the deposition of the Vedde Ash; some of them had already eroded the surface prior to the occurrence of the 11-10.8 cal ka cinder cones, but after the Preboreal Advance. The rupture of the Hnausar morainic arc developed more or less synchronously with the palaeolake formed during the 11.2 cal ka deglaciation, after the deposition of the Askja PB tephra (11.5 cal ka). The recent incision of the canyon was reaching the valley bottom probably prior to the infilling of the Younger Dryas glacial advance, but the re-incision by the Holocene floods had not yet been achieved at 11 – 10.8 cal ka, during the setting of the Askja S lava lake (Sigurgeirsson, 2016).

The Hólssandur fluviatile dunes are younger than the setting of the Askja S fissure eruption. The geochemistry of the dunes (samples Hols 1, 2, Table 2) yielded a Bárðarbunga source. It is very similar to that of the upstream fluviatile dunes at the foot of the Vaðalda Volcano (Dingjuvatn Dunes β) from which the northern termination resembles the Hólssandur fluviatile ones. Both dunes partly rework, and lap onto the orange loesses at Hólssandurthat included the Askja E Tephra (c.10.4 cal ka; Table 2, Hols 3). The only Bárðarbunga tephra that fit with this stratigraphy are those at 10.1 and 9.9 cal ka from the database (Table 1), the 9.9 cal ka event being the largest volcanic event (Guðmundsdóttir et al. 2016). The Hrossaborg terminal moraine remained strongly eroded by jökulhlaups that should fit the same event. The Kreppa terminal moraine (ca 9.3 cal ka) although eroded to the West was just pierced by a younger flood issued from the Kverka River related to a major volcanic eruption close to 9.2 or 9.1 cal ka from the Grimsvötn volcano. It probably corresponds to the event formerly described (Alho et al. 2005; Carrivick et al. 2013).

.

4.3 Skjálfandi–Fnjóskadalur

375 The valley of the Skjálfandafljót is a little-studied area (Figs. 2 and 9), but it is the regular path of
376 jökulhlaups (Björnsson, 2017). The upper valley is partly masked by the Middle Holocene lavas from
377 the Trölladyngja Volcano (< 4.2 cal ka; Sigurgeirsson et al. 2015; Fig. 2A).
378
379 *4.3.1 Lower Valleys of Skjálfandi and Fnjóskadalur*
380 This part is the most studied (Fig.8) on very few sections. We have thus described new ones and
381 analysed the tephra. The estuary has been ice-free since the Preboreal (11.2 cal ka; Norðdhal and
382 Pétursson 2005). The Bárðardalur Valley (Fig. 2A) was mostly incised in the bedrock, as close to
383 Fosshóll scabland, with lateral moraines bordering the lower valleys. Eemian, hyaloclasite-derived,
384 bioturbated marine deposits crop upstream out as pillars, along the valley bottom to 240 masl, from
385 the entrance of the lateral Fnjóskadalur.
386 At the eastern entrance to Fnjóskadalur, thick, massive deposits of fresh basaltic gravels are buried
387 under the recent loess along with the Askja S Tephra (11–10.8 cal ka; Fig. 10E). Inside the
388 Fnjóskadalur, the 'pitted' moraine at the western end of the lake (at Stórutjarnaskóli) is considered to
389 be from the Preboreal advance (Figs. 8, 9A; Ingólfosson et al. 1997). It is truncated by a terrace at 120
390 masl from the Fnjóskadalur palaeolake, but to the north, there is evidence of it being in a juxtaglacial
391 position, with iceberg thermokarst filled with fresh basaltic sands (Bárðarbunga, 11.3 cal ka, Table 1;
392 Table 2: Ljos2). These deposits also reworked an Askja tephra much older than the Askja S (Askja
393 PB, c. 11.5 cal ka), deforming very coarse, rounded gravel. It is usually covered by loesses, including
394 the Askja S tephra. The moraine morphology resembles the collapse features described by Fard
395 (2002) on jökulhlaup eskers, and by Olszewski and Weckwerth (1999) on sandurs. The lower alluvial
396 unit of the kame along the pitted moraine contains both reworked Vedde and Skógar Tephra (Table 2:
397 Ljos 1). Downstream of Fnjóskadalur, below Hólls, the side of the valley is pasted by lacustrine and
398 alluvial deposits resting on coarse till, including several layers of fresh basaltic sands reworking the
399 Vedde ash (Fig. 9C). These deposits are covered conformably by deformed loesses that incorporated
400 the in situ but deformed Askja PB Tephra at its base (c.11.5 cal ka; Fig.9E).
401 Two main morainic arcs are preserved in the parallel Aðaldalur Valley. The Fragarness arc is a
402 disrupted terminal moraine (Fig. 8). The related Palmholt Quarries (Fig. 8; Supplement Fig 4), host
403 broad, flat-bottomed kettle holes, which are invaded by deformed flood gravel layers and reworked
404 basaltic tephra. The morainic material is sandwiched between two generations of jökulhlaups, the

lower one reworking the Vedde tephra. The more recent generation accommodates decametric kettle holes. The late loessic sedimentation is similar to these of Fnjóskadalur including Askja Tephra. A later morainic arc, partly eroded, exists upstream, at the Laugar village.

4.3.2 Upper Valley, the Bárðardalur and Vosnaskarð depression

The morphology in the Bárðardalur Valley is only erosional and partly masked by Middle Holocene lavas from the Trölladyngja Volcano (< 4.2 cal ka; Sigurgeirsson et al. 2015; Fig.2B). Hníflar palagonite pinnacles are flood-sculpted in the central part of the Vosnaskarð depression (Fig.2B). A palaeolake occupied this depression, at a higher altitude (1100 masl) than the Vaðalda Volcano and palaeolake Hágongulón (see § 4.5).

Fresh glacial striae are oriented towards the Skjálfandafljót from the upper Sprengisandur (Fig. 2A). One terminal moraine is observed NW of Svartárvatn Lake, restricted to the right side of the canyon of the Bárðardalur Valley, a (Fig. 2A; Supplement Figs. 5A - 5B). The canyon was probably infilled by rather old tills and lacustrine deposits, as preserved on the left bank of the canyon at Halldórsstaðaskógur (Fig. 2A, Supplement Fig. 5C). Sandy basaltic deposits are splayed on the plateau, upstream and around the Svartárvatn Lake. The stratigraphy at Svartárkot clearly indicates a Bárðarbunga Tephra (probably 10.4 cal ka; Table 2), followed by the Reistvik 8 Tephra (10.2 cal ka; Guðmundsdóttir et al. 2016). SE of the Svartárvatn Lake, the Reitsvik 8 Tephra (Table 2, Svartár) is preserved in the upper part of the consolidated orange loess, but has been laterally eroded in a NE direction by jökulhlaups.

Another structure is visible to the NE of Svartárkot, on the plateau, near the Sellandafjall Tuya. These structure shaped the surface of the Kárkárbotnar Formation which is consolidated and faulted palaeofan considered as Late Glacial and initially scoured after the YD Advance (Sigurgeisson et al. 2015). An alluvial splay of granules and sands shaped the surface of Kárkárbotnar Formation into fluvial megadunes (two generations) and residual hillocks (Figs. 2A and Supplement 12) based on aerial views. This surficial morphology is associated with an esker (Fig Supplement.12 E) that propagated subglacially to Myvatn Lake from the north of Krákárbotnar, parallel to the present Kráka River. The final evidence of flooding is here the splayed sands stopping at the western foot of the Sellandafjell and associated with the sculpting of elongated islands in the loess cover

435 (Supplement.12). From these data, and the location of the terminal moraine in the Bárðardalur Valley,
436 the Kárkábotnar initial superficial scouring could be generated by the same events as these recorded
437 at the Svartárvatn Lake, a part of the flood(s) deriving towards the Myvatn Lake to the east (Fig. 2A).
438
439 4.3.3 Synthesis for Skjálfandi–Fnjóskadalur- Myvatn-Vosnarskard system
440
441 *Glacial advances and retreats*
442 In the Bárðardalur and Adaðalur Valleys, (Fig. 8), the basal fluvial sediments have reworked the
443 Vedde Ash as also observed at Laufas and Kaupangur in Eyafjörður (Sigurðsson and Sparks 1978;
444 Van Vliet-Lanoë et al. 2005). Ljosavatn and Palmholt quarries reveal dismantled glacier ice tongues
445 that represent a rapid advance or a surge. The Skjálfandi terminal moraine was located in the vicinity
446 of Skollahnjúkur as suggested by a perched pitted morphology at 200 masl (Fig.8). This surge can be
447 attributed to the "11.2 – 11.4 cal ka" Preboreal event (tephrostratigraphy; Ingolfsson et al. 1997),
448 formed before the deposition of the Askja PB and S Tephra. By deduction, the "10.3 cal ka" terminal
449 moraine could be restricted to these at the Laugar village. Upstream, the lateral moraine immediately
450 NW of Svartárvatn Lake most probably yields an age of ca 9.3 cal ka, based on tephra (younger than
451 the Reistvik 8 Tephra at 10.2 cal ka). This is the proposed Svartárvatn Advance.
452
453 *Jökulhlaups*
454 The oldest basal generation of flood immediately postdates the Vedde Ash and represents an early
455 stage in the Preboreal deglaciation. The main (second) generation of floods predates the Askja S
456 Tephra (10.8 cal ka), thus yielding 11.2 - 11.1 cal ka in age. The third generation took place before the
457 first Bárðarbunga eruption (10.4 cal ka; Guðmundsdóttir et al. 2016) and the overlying Askja E Tephra
458 (10.4 cal ka). The latter generation (last terrace) is logically related to eruptions of the Bárðarbunga at
459 c. 10.1 or 9.9 cal ka (Table 1; Guðmundsdóttir et al. 2016). Flood deposits from the Skalfandafljót
460 River were also washed into Fnjóskadalur and Eyjafjörður via the Dalsmynni Canyon (Hólls and
461 Finnastadir Farm; Figs. 4, 8D). This path for floods explains the water-lain facies of the “10.3 cal ka
462 Saksunarvatn Tephra” observed at Reitsvik (Guðmundsdóttir et al. 2016).
463 The surface granular components of the Krákárbotnar palaeofan (Sigurgeirsson et al. 2015) had
464 probably the same source and age as the deposits at Svartárkot, based on the orientation to the NE of

the megadunes. All these floods seem to issue from the Dingjujökull outlet glacier (Table 1, Fig.2B) and to correspond to the Bárðarbunga 10.4, 10.1 and mostly 9.9 cal ka tephra. These floods probably had a long duration (weeks or more), as they were mainly fed by deglaciation, justifying their lateral displacement to the east by the Coriolis force feeding the Myvatn basin. Re-incision in Preboreal glacigenic sediments of the Bárðardalur valley after the Preboral glacial advances occurred much later, prior to 7 cal ka, but probably from ca 9.3 cal ka.

4.4 Jökulsá á Brú and the East

4.4.1: Halslón palaeolake

To the NE of the Vatnajökull, sparse evidence of jökulhlaups has been recorded in the Halslón Dam sedimentary fill that was issued from the western Brúarjökull outlet glacier, via Kringislá (Knudsen and Marren, 2002). The stratigraphy of the Holocene events has evolved from the ones previously published (Knudsen and Marren, 2002; Van Vliet-Lanoë et al. 2010). The LIA moraine is located north of the Kringslaranni, on both sides of the dam lake, followed by successive termini. A terminal moraine older than the LIA is visible North of Hals, on the right bank of the lake (Fig.1b), fitting the 9.3 cal ka advance.

Jökulhlaups reworked first the Younger Dryas Grímsvötn Tephra, filling troughs with massive deposits (Van Vliet-Lanoë et al. 2010), that were further deformed by a first glacial advance. An Askja E Tephra (10, 2 cal ka comparable to Vestur R3 in Table 2; Fig. 7C) has been deformed by a second glacial advance. The Saksunarvatn Tephra was water-lain in the highest terrace and deformed as a thermokarst depression in a juxtaglacial position (Fig. 7D). Laterally, it is undeformed, and post-dated by a faulted geyserite at 10.09 ± 0.28ka BP (U–Th uncorrected dating; Van Vliet-Lanoë et al. 2007; Fig. 7E).

The Jökulsá á Brú River is deeply incised down from the Brú village, similar to the canyon of the Jökulsá á Fjöllum. Two remains of terminal moraines were preserved. Downstream, a ‘pitted’ moraine is visible on the left bank, at 1.5 km south of Selland, below a large mass flow on the right bank. This is probably an end moraine from the Botarheiði that evolved into a rock glacier. Further down, another 1.5 km long “pitted” end moraine crops out near Krókavatn (Fig. 1b).

4.4.2 The Eyabakkajökull

This glacial outlet shows traces of stacked, permafrosted ice-thrust ridges, comparable to several Svalbard glaciers (Boulton et al. 1999; Sund et al. 2009; Waller et al. 2012). They formed in relation with the 1890 surge and commonly attributed to hydraulic surging (Sharp, 1985; Kaldal and Vikingson, 2000; Björnsson et al. 2003; Schomacker et al. 2014, Fig. 11). The southern eastern part is a rather thin diamicton and associated with a negative inprint of ice crevices and a narrow sharp plastic edge and stacked folds of a surge fitting the 1890 one (Schomacker et al, 2014). The northernmost / outer part of this moraine seems to be partly older, seeing the thermal cracking and vegetation cover which are similar to the situation on the recent volcanic ridge at Veiðivötn (1477 AD eruption). For the nearby Brúarjökull Glacier, the presence of a glacier-deformed Öræfajökull Volcano pumice (1362 AD eruption; Benediktsson, 2012) suggests a setting during the coldest part of the Little Ice Age, from 1600 AD to 1800 AD (Guðmundsson et al. 1997). The Mülajökull Glacier had its maximal advance between AD 1717 and 1760 (Benediktsson et al. 2015). The persistence of relict morainic arcs within a palsa bog immediately downstream of the Eyabakkajökull terminal should indicate a long, unglaciated interval, at least from the 9.3 cal ka advance. Furthermore, a field of open-system hydrolacolite occupies the western side of the valley, attesting of the limited glacial extent to this side. Several jokulhaups have pierced the arc, mostly to the West, in association with an esker, but it does not seem possible to build a chronology.

Observations were performed downstream at the Lögurinn Lake (Fig. 1): the deglacial sedimentation covered an interval from 10.2 cal ka (Strinberger et al. 2012; Guðmundsdóttir et al. 2016; Norðdahl et al. 2019), fitting an age of 11.2 cal ka for the terminal moraine north of Eglisstaðir (Fig. 1).

4.4.3 Synthesis.

Glaciers

At the Halslon Lake, the older Grímsvötn Tephra has been reworked in flood troughs in association with the Bölling deglaciation (Fig. 10). The Boreal advance is slightly younger than 10.4 cal ka (Askja E Tephra) at the foot of the Kárahnjúkar Tuya (Fig. 7C). This corresponds to a “10.3 cal ka” advance, synchronous with the Hrossaborg and Laugar events. Laterally, the "9.3 cal ka" terminal moraine from the Brúarjökull Glacier reached the deformed Saksunarvatn Tephra in the middle of the length of the Halslón Lake, equating with the Kreppa–Svartarvatn Advance to the west.

To the East, the Eggilstadir moraine yields c. 11.2 cal ka. The moraines relics in the palsa bog thus yields c. 9.3 cal ka; the outer Eyabakkajökull stacked vegetated moraine with ice wedging and thermokarst (mostly to the East) yields a LIA age and the Eyabakkajökull thin recent stacked moraine yields a 1890 AD age.

Jökulhlaups

Megafloods first seem to occur prior to the YD. The Saksunarvatn Tephra splayed in a flood, being preserved intact in juxtaglacial position from a pre-existing surge lateral moraine, yielding probably c. 10.3 cal ka.

4.5 The South-West: The Þjorsá–Kadakvísl–Tungnaá outlet

The South-western main outlet from the Vatnajökull is drained by at least 3 valleys (Fig.1a). The Þjorsá–Kadakvísl–Tungnaá Valleys are clearly shaped by jökulhlaups over the last two interglacials (Van Vliet-Lanoë et al. 2018). This is proven by the occurrence of floods erosional forms (Supplement Fig.6). The Late Glacial sedimentary prism is rather thin, mostly located in the jökulhlaup incisions, sometimes infilled with sediments associated with the tidal deposits of the Preboreal marine transgression. Regional field descriptions are rare, and most of the data are being extracted from lake cores (Geirsdóttir et al. 2009). To the north of this system, data are non-existent or unpublished.

4.5.1 Akbraut and Varghóll Quarries

The section at Akbraut (Figs 1, 10) is located on a terrace perched at 90 masl on the east bank of the Þjórsá River. It is situated south of the Búði moraine complex, dated at ca. 11.2 cal ka (Geirsdóttir et al. 2009), and north of the Pula–Mykjunes terminal moraines (YDII, in situ Vedde Ash; Van Vliet-Lanoë et al. 2018). It has an infill of coarsely-stratified, unsorted and unconsolidated cobble material, set by jökulhlaups, which are incised into the Eemian and Weichselian deposits. These gravels are covered by stratified lacustrine silts, deformed by moderate seismic activity, as is also the case in the section at Hrepprhólar (Fig. 1), where they are related to Termination Ia. A second unsorted diamicton was deposited, which includes, at its base, fresh, dark basaltic sands that are coarsely stratified, and sheared by glaciotectonism (Vedde β, 11.8 cal ka, Van Vliet-Lanoë et al. 2019). This is covered by 1

553 m of stratified marine silts (from Termination Ib), including Vedde pumice-rich beds, with small load
554 casts. This marine unit is further truncated by more recent jökulhlaup gravely deposits.
555
556 The Varghòll–Akbraut moraines correspond, in aerial view, to thin terminal moraines that are later than
557 the YD, but older than the major Búði terminal moraine. These moraines present surge-type
558 characteristics, with a stacked folded pattern. The suggested age, from the presence at the base of
559 reworked Vedde Ash, is ca. 11.4 – 11.3 cal ka, followed by the 11.2 cal ka Búði Advance.
560 To the West, “pitted” jökulhlaup abraded rocks (Supplement Fig. 7) crop at 230 masl on the Skarðsfjall
561 (Fig.1A), disconnected from the natural drainage system. It suggests a discharge of water emerging
562 from the surface of a thin decaying glacier lobe during the late YD or the Early Preboreal, probably
563 from a crevice net.
564
565 4.5.2 Upstream watershed of Þjórsá River
566 Another terminal moraine was mapped by Kaladal and Vikingsson (1990) to the north, east of the
567 Sultartangalòn Lake. It is associated with an eroded esker deposit (Fig.12A). Herein, this terminus will
568 be referenced as the Búðarhals Advance. At the hydroelectric station of the Þjórsá Lake, the base of
569 the Late Glacial to the Holocene canyon infill is extremely rich in basaltic tephra, resting on an Eemian
570 fluvial formation, as in the Upper Ytrí–Rangá Valley (Van Vliet-Lanoë et al. 2018).
571 Upstream, the Þjórsa River is connected to the artificial Hágögulòn Lake (Fig. 1A). This lake’ site was
572 occupied several times by palaeolakes. At the eastern foot of the Nyðri Háganga Tuya, ca. 100 m
573 above the original valley floor, the upper raised beach (at 887 masl) is covered by scattered fresh
574 basalt fragments that were issued from the Bárðarbunga Volcano. This upper raised beach is at the
575 same altitude as the tephra filled Vaðalda crater, east of the Askja Volcano (Figs 1, 2B). Another
576 palaeolake outlet is perched at 860 masl, and is connected to a lake level located at 80 m above the
577 valley floor, associated with a retrogressive dry valley, incised in an Eemian glaciofluvial deposit
578 (Supplement Fig. 8E). Many jökulhlaup-polished blocks (Supplement Fig. 8A-D) are visible at 835
579 masl, 65m above the valley floor, at a palaeo-outlet of the palaeolake. It seems that this palaeolake
580 infilled several times, with up to 100 m of water for the oldest highstand, with evidence of flood
581 bursting (incision). Damming was generated by westward ice surging from the Tungnaárjökull and
582 Sylgjujökull outlet glaciers (Fig. 1, extent in yellow). This is evidenced by the morainic system that

583 ends close to the Kisa River to the west (Fig. 7C; Kaldal and Vikingsson 1990), issuing from the north
584 of the Sauðafell hill (North of Veidivötn). This is associated with evidence of lakes with terraces, and a
585 field of open system pingos in silty sands, close to 850 masl, at SW of the lake. It is overlapped finally
586 to the south by the Þjórsa Lava (8.6 cal ka). This terminus will be herein referenced as the Kisa
587 Advance, surging from the Tungnaárjökull and Sylgjujökull outlet glaciers.
588
589 4.5.3 Synthesis for the Þjorsá–Kadakvísl–Tungnaá outlet
590 Following the Glacial Termination Ib, several glacial advances occurred in the south. The twinned
591 advances of the YD I – Pula moraine (c. 12.8 ka cal) – and YD II– Mykjunes moraine (c. 11.7 – 11.5
592 cal ka) – formed a major glacial terminus (Van Vliet-Lanoë et al. 2018).
593 Observations at Varghóll suggest a retreat from Mykjunes to the Búði arc, with pulsed surges
594 associated with jökulhlaups and iceberg discharges (Figs 10, 11) that correlate with a c. 11.4 – 11.3
595 cal ka surge, the Varghȯll – Akbraut Advance just after the YD deglaciation. The Búði Terminus fits the
596 "11.2 cal ka" Preboreal advance (e.g. Geirsdóttir et al. 2009). The next glacial advance should
597 correspond, in the south, to the Búðarhals Advance on the eastern side of the Kaldakvísl River. A later
598 trace of glacial surge emerges from the East, between the Sandfell in the south and the Hágöngulón
599 lake sector in the north, to the Kisa River, but this seems to have been untouched by jökulhlaups. Its
600 source was hindered by the Þjórsá Lava, at 8.7 cal ka (Halldórsson et al. 2008), and seems to have
601 issued from the Syglujökull and Tungnarjökull outlet glaciers, which normally surge westward
602 (Björnsson et al. 2003). This places at ca. 9.3 cal ka cal the Kisa Advance which is an erratic advance.
603 This indicates an age of ca 10.3 cal ka for the Búðarháls Advance.
604
605 **5. Discussion**
606 To understand the various potential controls on jökulhlaup genesis, we first discuss the climate
607 evolution and deglaciation history for each outlet of the Vatnajökull. Second, we analyse the
608 connection between glacio-isostasy and the potential storage of aquifers, or of subglacial lakes, at the
609 level of the Vatnajökull. On this base, it will be possible to discuss the dynamics that drove the Early
610 Holocene jökulhlaups.
611
612 ***5.1 Timing of the Glacial Advances*** *(Fig.1 b)*

After the deglaciation of the YD and the deposition of the Vedde ash (ca 11.8 cal ka), the Early Holocene glacial advances of the Vatnajökull spreaded at ca 11.5-11.4, 11.3-11.2, 10.3 and 9.3 cal ka, in concert with climate evolution in the other regions surrounding the North Atlantic (see § 3.1.).

The Varghòll – Akbraut in the South, Hnaussar, Ljósavatn and the Fragarness - Palmholt terminal moraines in the North (ca 11.4 - 11.3 cal ka) correspond to the first Early Preboral advance. The Búði (c. 11,2 cal ka) is a second Early Preboreal Advance. The later Búðarhals Advance in the South is estimated to be synchronic with the Erdalen Events and the Saksunarvatn complex tephra, at c.10.3-10.2 cal ka as well as the Hrossaborg, Laugar and Eglisstaðir termini in the North. For the independent Langjökull on the West Volcanic Zone, the Saksunarvatn Tephra has been found below a lava flow (Jóhannsdóttir 2007; Eason et al. 2015), also suggesting an early deglaciation, and isolation of the southern and eastern margins of the glacier.

The Kreppa, Kisa, Svartárvatn and outer Eyabakkajökull Advances seem to be equivalent to the “9.3 cal ka” Cooling Event. They are characterized as erratic in their flow direction, compared to the Late Glacial and Preboreal Advances. This late advance is also recognised around the Drangajökull Glacier (NW peninsula; Harning et al. 2016).

The “8.2 cal ka” event has not been officially recorded in lacustrine records in the NE of the island (Striberger et al. 2012); however, it is clearly recorded in cores at Hvitarvatn (Langjökull; Larsen et al. 2012; Fig. 1) and is also extractable from the ^{3}He measurements of volcano summit lava’s tracing the local deglaciation (Liccardi et al. 2007). This means that the glacial limits for this pulse were mostly inside the present extent of the glacier.

5.2 Timing of the Jökulhlaups *(Fig.2 B)*

In the Jökulsá á Fjöllum, major jökulhlaups thus occurred from our data in relation to the Younger Dryas deglaciation (Hnausar kame terrace), probably between 11.8 and 11.4 cal ka, centred on 10.1 – 9.9 cal ka (Hölssandur) and ca 9.1 cal ka south of the Hrossaborg. The major Icelandic jökulhlaups in the literature relate to the onset of canyon clearance of the sedimentary infilling. After 9.3 cal ka, some events were still large, but were better channeled.

It thus seems that most of the early jökulhlaup events in the Þjórsá, Skalfandi, Jökulsá á Fjöllum and Jökulsá a Brú valleys occurred from the Late Younger Dryas deglaciation, some having bursted just prior to the Early Preboreal Advance (at 11.2 cal ka). The jökulhlaup mentioned at Kjölur (Kajafell

643 Volcano, Langjökull) by Tómasson (1973) also seems to correspond to a first-generation surge (at
644 12.0 to 11.2 cal ka), as it is associated with iceberg kettle holes and two eskers, all overflowed by the
645 Preboreal lava (Eason et al. 2015).
646
647 In the South, after the Preboreal, the majority of flood events occurred after the Búðarháls Advance
648 ("10.3 cal ka"), but prior to the Kisa Advance (" 9.3 cal ka"). These field data fit the results from the
649 Hestvatn Lake record (Fig.1; Geirsdóttir et al. 2000) that assigned two major periods to the flood
650 activity around 12.0 - 11.2 cal ka, and again around 10 – 9.9 cal ka as it is also the case for the
651 Jökulsá á Fjollum watershed.
652
653 ***5.3 Permafrost and surging***
654 Outlet glaciers of ice caps that periodically surge after long quiescent phases, undergo large and
655 sudden pulses accompanied by terminus advance (Harrisson et al. 2015; Benn et al. 2019).
656 Polythermal glaciers, often associated with permafrost are prone to slow surging (Benn and Evans,
657 2011). The temperate glaciers in Iceland exhibit surges with a sudden onset, extremely high (tens of
658 meters/day) maximum flow rate and an abrupt termination, associated with a discharge of the intra-
659 glacier stored water (Björnsson et al. 2003). It can be triggered by an enhanced climate-driven melting
660 (Stiberger et al. 2011) or a volcanic meltwater supply. Ice breakage at the glacier surface or perched
661 outlets, with the local surface dismantling and iceberg splay, can be induced by constrained
662 overpressure (Roberts et al. 2000). The downward locking of hydraulic pressure can result from the
663 impeded drainage by permafrost development that seals the snout and margins of the glacier, frozen
664 to the bed during cooling events, as in the polythermal glaciers in Svalbard (Fig. 12D; Lonne et al.
665 2016).
666 The impact of the permafost seems evident for the Eyarbakkajökull outlet and the Kreppa, Kverká and
667 Jökulvisl River outlets of the Brúarjökull Glacier (evidenced by the recently pitted terraces). This
668 system with surface dismantling is also valid for the outlets of the Breiðamerkurjökull River, in
669 association with concertina eskers (Knudsen, 1995), for the Gígjulvísl and Skeiðará Rivers
670 (Skeiðarárjökull Glacier) and the uppermost Tugnaá River.
671 As the Preboreal climate was rather cold especially during the two first Bond events, particularly in the
672 North-East (about - 10°C lower than today; Rasmussen et al. 2011), we might expect the impact of

permafrost damming to be one of the main triggers of jökulhlaups.The preserved pre-jökulhlaup morphology suggests such permafrost prior to the principal Early Holocene flood, also deformed by tectonic faulting to the east (Fig. 14C). The degradation of ice bodies in the terminal moraine during a warming event could have reduced the internal stability of the dam and, therefore, easing flood emergence (GAPHAZ 2017). Sealing of the glacier tongue by permafrost could have favoured the retention of meltwater in the subglacial lakes or intraglacial aquifers, especially if the surface and bottom slopes were very low (see § 5.2), increasing the probability for glacial surging for both polythermal and temperate glaciers (Benn et al, 2019). Proglacial icing accumulations from eskers could also have induced damming. This was likely the case for the glacial tongues reaching the lower Skálfandi River (at Ljósavatn and Palmholt) and the lower Þjórsá River (at Varghóll), around 11.2 cal ka. After 10.4 cal ka, jökulhlaups were largely splayed on the deglaciated plateaus, The occurence of permafrost in the watershed probably limited the vertical incision of any flood, promoting a lateral extension of such floods in the valleys, as it took place with the first mega-jökulhlaup, responsible for the Hólssandur hydraulic dunes (Jökulsá á Fjöllum), or the Svartárvatn–Krákárbotnar jökulhlaup (at Skjálfandafljot).

5.4 Impact of the glacio-isostatic rebound

As the c. 10.8 cal ka Askja S Tephra and the c. 10.3 cal ka Saksunar events happened relatively soon after Termination Ib, an early glacial rebound from the coast to the inland, should be expected attenuating the slope of the lower to middle Jökulsá Valley. The distance from Röndin to the Hrossaborg moraine is about 50 km, and is being uplifted at rates similar to those in the south of the isle, c. 40 to 60 mm yr^{-1} (Le Breton et al. 2010). Present-day isostatic uplift around the Vatnajökull is 9 to 25 mm yr^{-1} (Pagli et al. 2007). The persistence upstream of an extended Vatnajökull suggests that this sector is still downwarped in relation to the remaining ice thickness, and the presence of the hotspot (due to lower viscosity). An initial subsidence of 500 m is expected at the LGM for a 1500 m thick ice sheet. Supposing that half of the ice-sheet thickness (ca. 750 m) has already melted at 10.3 cal ka, we could theoretically expect a residual subsidence of 250 m in the central part of the system, and half of that (125 m) in the outlet zone of the Hrossaborg and Buðardalur surging tongues. This simple but certainly overestimated approach allows imaging of the potential extent of subglacial lakes or aquifers (Fig. 13) which are retained below the residual thinned flat ice-sheet (slope ca 4%,

703 subglacial volcano excepted), and adapted from the subglacial topography described by Björnsson
704 (2017). Due to the speed of the rebound (ca 25 - 40 mm yr-1 from the present-day values) imposed by
705 the fracturated substratum (Höskuldsson et al. 2006; Le Breton et al. 2010), this isostatic rebound had
706 very little chance of strongly modifying the geometry of the meltwater catchment areas for the brief
707 interval (10^2 yrs) considered, but the isostatic subsidence was certainly resorbed after 1 ka, as in the
708 "9.3 cal ka" deglaciation.
709
710 ***5.5 Volcanic activity, jökulhlaups and unloading***
711 Glacial unloading could directly influence the activity of volcanoes by adiabatic crustal melting
712 (Eksinchol et al. 2019). The Grímsvötn and Bárðarbunga Volcanoes were partly merging from the ice
713 sheet since 18 cal ka and mostly from 11.8 cal ka (Van Vliet-Lanoë et al, 2019). With the ongoing
714 rapid warming from 11.8 cal ka (Fig.3), the glacial unloading of the western Vatnajökull allowed the
715 supply in magma in the deep subcrustal reservoirs of the NVZ and EVZ (Hartley and Thordarson,
716 2013). This supply fed first the Grímsvötn and Bárðarbunga reservoirs (see tephra record, Table 1).
717 The Askja Volcano is presumed deglaciated around 10.3 cal ka only (Hjartarson, 2003; Hartley and
718 Thordarson, 2013), but it was fully emerged from 11.4 cal ka. The PB Tephra was followed several
719 smaller eruptions (Fig.10; See Supplement Fig.4), before the major Askja S. The Saksunarvatn
720 Tephra (10.24 – 10.12 cal ka) has a more complex story.
721
722 The potential triggering effect on eruptions of small unloading events, such as water discharge from a
723 lake and ice thickness variations, has been demonstrated when the underlying magma chamber is
724 close to failure conditions comparable to the static stress change induced by earthquakes (1-10 kPa;
725 Albino et al. 2010). Today, ice loss reaches 6 m yr^{-1} for the Vatnajökull (http://Vedur.is). The climatic
726 unloading reaches 60 kPa after 100 years of warming, with a potential effect on the upper reservoir of
727 the Grímsvötn Volcano.
728
729 Thermal analysis at the Kverkfjöll Volcano has indicated that a jökulhlaup must have taken place a few
730 days after the initial subglacial lava emplacement (Höskuldsson et al. 2006). Maximal ice melting rates
731 of the order of 10^3 m s^{-1} have been indicated. The magma must have reached water content close to
732 saturation at emission allowing the onset of a phreatomagmatic eruption after lake drainage

733 (Höskuldsson et al. 2006). It also lowered the melting temperature of magma and the spreading of
734 extensive lava flows (Wylie et al. 2000), as observed immediately after deglaciation. This interpretation
735 suggests that jökulhlaups reactivate eruptions by lowering the pressure on the magma chamber
736 (Höskuldsson et al. 2006; Albino et al. 2010).
737
738 The expected succession for deglacial events are thus: 1) subglacial eruption; 2) lake formations; 3)
739 jökulhlaup and iceberg discharge, or possible glacial surge; and 4) phreatomagmatic ash emission.
740 This succession could occur rather rapidly, within a few weeks, or be recurrent as a part of the 10-year
741 cycle for Grímsvötn volcanic activity and is most likely for summer events, especially if the perturbation
742 is within a range of 7 kms from the centre of the reservoir (Albino et al. 2010). Climatic glacial
743 unloading, at present values, seems to be enough to induce a first eruption of the upper reservoir.
744
745 *5.6 Climatic melt control and jökulhlaups*
746 Jökulhlaups have been recorded from the Alleröd cooling (ACE Fig.3), even during brief events in the
747 Younger Dryas, especially in the NE of the isle, commonly starved in precipitation. The onset of
748 warming would have raised the water level in subglacial lakes, favouring surges (e.g. Russell et al.
749 2001). From 10.25 cal ka BP, warming was significant, producing temperatures similar to those of
750 today (see § 3.1). Restoration of the Irminger Current favoured a rise in precipitation. Rapid ice melting
751 could have been driven by intense late-summer rainfall, causing the thinning of large ice-sheet at low
752 altitudes (Doyle et al. 2015). Surface melt-lakes represent today ca. 1 km^3 of the decaying part of the
753 Greenland ice-sheet (Fitzpatrick et al. 2014). The depression below the Brúarjökull outlet glacier
754 (Brúarjökull Lake; Fig. 16) is the largest, but with an "impermeable" bedrock. This glacier surged first.
755 Traces indicate that surging certainly issued from the west of the Brúarjökull in both of the latter
756 events, the "10.3" and "9.3 cal ka" ones. The surge responsible for the Hrossaborg Advance ("10.3 cal
757 ka") clearly dammed from the north the depression south of the Vaðalda and Askja Volcanoes. This
758 explains the Dingjuvatn Dunes and the splay of dark tephra on the western flank and in the crater of
759 Vaðalda, to 200 m above the valley floor, emitted by ca 10.1 and/or 9.9 cal ka eruption of the
760 Bárðarbunga. The Kreppa Advance ("9.3 cal ka") mostly dammed the Jökulsá á Fjöllum, and was
761 probably responsible for the high flood described by Alho et al. (2007). Both flood series (c. 10.1–9.9
762 cal ka and < 9.3 cal ka) were initially linked to ice-damming. Today, most outlet glaciers in Iceland are

763 thin, plastic and temperate-based surging glaciers (Bjornsson, 2017). These could be more
764 susceptible to recurrent overpressure compared to the colder surging glaciers (Ben and Evans, 2010)
765 that existed in Northern Iceland during the Preboreal and that probably needed higher overpressures
766 to breach a permafrosted dam.
767
768 As the '10.3 cal ka' events seem to have been rather synchronous with the Askja, Grímsvötn and
769 Bárðarbunga eruptions, a supplementary melt is expected from the splay of ash on the surface of the
770 glaciers. A lowering of surface albedo could have further increased the melting efficiency by 60%
771 (Vogfjörd et al. 2005; Möller et al. 2013). The low albedo measured in 2005 is related to the 2004
772 Grímsvötn eruption (Möller et al. 2013) that was immediately followed by a jökulhlaup (Vogfjörd et al.
773 2005). This is also valid for the Gjálp eruption in 1996 (Guðmundsson et al. 1997; Björnsson, 1998;
774 Russell and Knudsen, 1999). Insolation has been rising since 10.29 cal ka, to a high between 10.20
775 cal ka and 10.05 cal ka, with a maximum value of ‰ $\delta^{14}C$ at 10.13 cal ka (Stuiver et al. 1998; Fig.2),
776 enhancing ice sheet collapse. Intervals of positive mass balance for the glaciers have conversely
777 lowered the volume and frequency of recent jökulhlaups (Guðmundsson et al. 1995). It thus seems
778 that the first large eruption took place subsynchronously with the breakage of the ice-dams north of the
779 Vaðalda, at ca. 10.2 cal ka, in agreement with ice-core dating. The Bárðarbunga Tephra, observed at
780 the base of the Svartárkot Tephra sequence, probably fit the ca 10.45 cal ka event (Guðmundóttir et
781 al. 2016), or possibly another event closer to 10.25 cal ka, masked by the volume of Saksunarvatn
782 Ash. In the following years, insolation rose to a maximum, and melting was enhanced by the first large
783 ash splay. Local eruptions blasted from Grímsvötn with the discharge of the caldera lake, with a
784 frequency close to the usual 60-year cycle during the century to 10.12 cal ka, thus filling the subglacial
785 lakes.
786
787 ***5.6 The complex history of the Saksunarvatn event and associated jökulhlaups***
788 *Phase 1 – Glacial rupture and lake drainage ca. 10.3 cal ka*: the aerial Vaðalda Lake (Fig.10) was ice-
789 dammed by the surge of the Bruarjökull (Kreppa advance, to 200 m water depth) and fed by climatic
790 melt. But it is too far from both the Grímsvötn and Bárðarbunga Craters to have influenced the
791 reservoirs mechanically. Subglacial lakes as the Brúarjökull Lake or aquifers, also climate-fed, have
792 expanded probably to the edges of the Grímsvötn caldera. An initial breaching or lifting of the

permafrosted glacier margin down from the Vaðalda Lake, followed by the drainage of subglacial lakes / aquifers may have been associated with unloading and the first volcanic event, close to the cold Erdalen Events – “10.3 cal ka” – in relation to the shallowest magmatic chamber. The other possibility also exists: with this subglacial eruption, the input of warm water would have increased suddenly as today (Snorrason et al. 1997; Björnsson 1998; Russel et al. 2002), the subglacial water pressure, allowing hydraulic fracturing, buoyancy and subsequent ice-dam rupture.

Phase 2 – Main volcanic activity ca. 10.25 cal ka: Based on the sizes of the Brúarjökull and Vaðalda Lakes, it is plausible that the deepest reservoir at Grímsvötn could have been triggered by this forced drainage, promoting the main phreatomagmatic ash eruption, the main Saksunarvatn event and the Skeidarar jökulhlaup (Lacasse et al. 1998). Massive basaltic ash deposition occurred during the diminution of the flood, and on all the slackwater deposits along the upper Jökulsá á Fjöllum Valley. The drainage of the caldera to the south (via the Tungnaá River) probably occurred with a second eruption, as similar to the occurrence of the delayed triggering of the Bárðarbunga eruption (at 10.15 cal ka). Several high floods thus emerged during the ca 10.24 – 10.15 cal ka period in the whole Jökulsá Rivers of the Vatnajökull. Furthermore, these events seem to have had a limited erosional capability, probably due to low-angled slopes and the persistence of permafrost, particularly during the Preboreal.

Phase 3 – The Bárðarbunga and Grímsvötn late response, 10.15–9.9 cal ka: The 10.15 cal ka eruption of the Bárðarbunga Volcano occurred in a similar way to that at Grímsvötn (10.25 cal ka) – by the disturbance of deep magmatic reservoirs. This interpretation probably also fits the ongoing deglaciation between the volcano and the western Tungafells outlet glacier, allowing massive storage in the natural-aerial Hágöngulǫn and Vonarskarð Lakes (Fig.13), resulting in flood escapes through the Vonarskarð Lake to Skjálfandi. Icebergs were apparently included in the jökulhlaup deposits, along with ash-rich deposits from the slack waters. The major jökulhlaup at 9.9 cal ka had already occurred by the onset of the next cooling, due to insolation, and is recorded in the Þjórsá Valley on the Akbraut 90 m terrace (last superficial event; Figs 1,10), at Hǫlssandur (Kvensodull dunes) and at Dingjuvatn (close to the Askja), as also in surface the Krákárbotnar palaeofan (Bárðarbunga source).

5.6 Hypothetical mega-jökulhlaups

The two potential mega-jökulhlaups were those (1) responsible for the limited Varghóll surge (South, ca. 11.5 cal ka) and the Hnausar surge and bursting (Jökulsá á Fjöllum; ca. 11.5 cal ka) and (2) the "Hólssandur hydraulic dunes" event (Jökulsá á Fjöllum, Barðardalur, Þjorsá Rivers; ca 10.1–9.9 cal ka). These were of the rupture type, with a permafrost infiltrated terminal moraine.

Volcanic melt-induced floodwaters were likely rapidly transmitted down via fractures nets in the ice and the bedrock, with peak flooding lasting only for a few days (Björnsson, 1998). In the case of the climatic-melt-and-ice-rupture type, the lake discharge increased slowly to reach peak flow. Such floods are cold, dense and progressive (Snorrason et al. 1997; Flowers et al. 2003) in connection with climate warming. They probably took a much longer time to diminish, due to the more diffused geometry of the path of subglacial water migration. If a diffuse aquifer was formed, constrained by permafrost, the duration of the drainage might have been several weeks, limiting the size of the maximal outburst.

Evidence for large prehistoric peak discharges of 0.2 – 1.0 10^6 m^3 s^{-1} in the Jökulsá á Fjöllum Valley has been presented by Sæmundsson (1973), Tómasson (1973, 2002) and Waitt (2002), among others. For the upper valley, Alho et al. (2005) and Carrivick et al. (2013) estimated a maximal discharge of up to 0.9 10^6 m^3 s^{-1} along the entire Jökulsá á Fjöllum for the "9.3 cal ka" events. At the level of Hrossaborg, we obtained a peak discharge of 0.71 10^6 m^3 s^{-1} to erode its top (50 m water depth) by using the flood-affected transverse profile of the valleys and the same flow speed (Alho et al. 2005: 2.0 m s^{-1}). Modeling by Gylfadóttir et al. (2017) estimated a flood discharge of 0.1 10^6 m^3 s^{-1}, for a flood level at the footh of the Hrossaborg. At the level of Hólssandur (Kvensodull, 10.1 – 9.9 cal ka events), we obtained a peak discharge of 1.65 10^6 m^3 s^{-1} with the present-day morphology, and 1.08 10^6 m^3 s^{-1}, assuming an infilled canyon to 200 masl (Hólmatungur–Vestudalur terrace). At Ásbyrgi, Waitt (2002) estimated it to be 0.7 10^6 m^3 s^{-1}. Our observations give a similar value for an infilled canyon.

The Preboreal jökulhlaups in Iceland were not much bigger than the others, or for the Jökulsá Rivers, not largely exceeding a maximal volume of 1 10^6 m^3 s^{-1}. This implies a limited significance for climate-

853 driven meltwater storage in subglacial aquifers and lakes, and their specific drainage contributions, as
854 also stressed for the recent warming (Flowers et al. 2003). Since the volume of the Bárðarbunga
855 caldera is 3.6 10^6 m^3, the emptying of this basin is not sufficient to provide such a discharge for hours,
856 but it obviously contributed to flood peaking. The volume of climate-driven meltwater has in turn
857 impacted the loading / unloading of magmatic chambers to trigger eruptions, controlling the maximal
858 discharge of floods obviously much less than do volcanogenic events. All volcanic / climatic
859 combinations are possible, but during deglacial times, the duration of flood events was probably very
860 long, of the order of a few months following the season. For these reasons, they seem less efficient as
861 a bedrock erosion agent than commonly published. This is not true for soft sedimentary infillings.
862
863 The canyons incisions for the different outlets of the Vatanjökull result apparently from recurrent
864 periods of activity throughout the Quaternary. This is shown by the preservation of the very old and/or
865 last interglacial sediments close to the valleys bottoms. The excavation of the successive
866 unconsolidated glacial infills, perhaps reached several times the basement during the early Holocene.
867 The Bárðardalur sedimentary infilling was fully re-excavated before the Svartarvatn advance (ca 9.3
868 cal ka). The Jökulsá á Fjöllum valley already was deeply excavated prior to the re-infilling by the
869 Preboreal advance (ca 11.3 cal ka); the last re-excavation started with the ca 9.9 cal ka event, as
870 probably also in the Bárðardalur. It corresponds to the largest splayed jökulhlaups in connection to the
871 ca 9.9 cal ka major eruption of the Bárðarbunga Volcano (Guðmundsdóttir et al. 2016) and perhaps
872 the emptying of the whole caldera: a profond channel scours the northern side of the caldera
873 (Björnsson, 2017). The ^{3}He dating provided by Baynes et al. (2015) of the surface exposure of the
874 terraces from the “9.9 cal ka” event represents the clearance by steps of the Jökulsá á Fjöllum valley.
875 This erosion within the canyon is more efficient to incise the basement due to constricted floods.
876
877 5.7 Generalisation
878 The expected succession for deglacial events is not the systematic rule. A subglacial major eruption is
879 rarely immediately followed by the formation of a large lake, a surging in form of jökulhlaup or glacial
880 surge and a final emission of phreatomagmatic ash. Some steps are often missing or delayed in time.
881 The Preboreal megafloods revealed in Iceland that climate-driven flood events from ice-cap internal
882 storage are generaly long, with relatively limited discharges, but potentially large volumes. This can be

883 compared to dam breakage as for the Missoula Lake (Wait, 1985) or for the Proglacial Lake in Altai
884 (Rudoy et al, 1993). The piking of the flood discharge occurs as well with dam breakage as with
885 subglacial eruption. Surging of glaciers is frequent today as in Preboreal times. These floods are
886 generally associated with major deglaciation events, excepted when the subglacial volcanic activity is
887 raised by a major glacio-isostatic unloading. Wide water lateral-splay are most probably linked to
888 permafrost persistence in the valley and do not necessarily imply larger flood volumes.
889 The canyons incision are for a major part an inheritage of quaternary glaciations.This morphology is
890 commonly recycled with recurrent glaciations, following the same flow lines. It has been also
891 demonstrated for the ice-dammed Missoula Lake (Waitt, 1985; Clague et al. 2003). The erosion
892 capability of megafloods have been exaggerated, even more efficient in constricted conditions.The
893 youngest incision in glacigenic environment proceeds by clearance of the successive glacial pulse
894 accompanying the deglaciation under control of the glacio-isostatic rebound. Only the full interglacial
895 flows will incise efficiently the bedrock.
896
897 **6. Conclusions**
898 Deglaciation events are almost synchronic in Iceland with the surrounding north Atlantic regions, as far
899 the accuracy of the dating may allow correlations; they are under control of the Irminger Sea Current.
900 The Preboreal jökulhlaups in Iceland fully correlate with both the deglaciation events and the
901 subglacial volcanic activity. This succession, initially triggered by climate change, and responsible for
902 superficial melting and volcanic activity, led to cascading retroactive events. The succession occurred
903 at least twice close to 11.5 – 11.3 cal ka and around 10.3 to 10.1 – 9.9 cal ka. Minor events existed
904 during the Alleröd / Younger Dryas, and also probably occurred in association with the “9.3 cal ka”
905 deglaciation, with an already restricted ice-cap mass. These Preboreal jökulhlaups were not much
906 larger than the others, and never largely exceeded a flood of 1 10^6 m^3 s^{-1}. They splayed on partially
907 frozen ground with a limited incision capability, often driven to the East by the Coriolis forces. Ongoing
908 glacial rebound to 10.3 cal ka temporarily lowered the slopes of the valleys, limiting the clearance and
909 incision of the canyons. The Saksunarvatn Tephra mostly marked the end of the main phase of
910 deglaciation, at 10.3 – 9.9 cal ka, in relation to the temperature rise to the thermal optimum. It also
911 signaled the onset of interglacial activity for the Barðarbungá and Grímsvötn Volcanoes. These close
912 interrelations between climate and volcanic activity for generating jökulhlaups of long duration during

913 major deglaciations events can be easily applied to other volcanic englaciated regions such as
914 Western Antarctica, Alaska or Oregon.
915
916
917 ACKNOWLEDGEMENTS
918 This study was funded by the French Polar Institute Paul-Emile Victor (IPEV), Arctic Research
919 Program number 316 (ICPROCI I, II and III), which covered the fieldwork in Iceland. We especially
920 thank - Kristjan Sæmundsson for providing the original dating for the Krafla caldera and - the
921 Vatnajökull National Park to have allowed investigations and samplings in protected natural areas. We
922 also thank the students Anne-Sophie Van Cauwenberge, Audrey Wayolle, and Guillaume Gosselin for
923 their assistance during fieldwork in 2004, 2006, and 2008. We also gratefully thank a reviewer for all
924 his positive comments and suggestion of improvements.
925
926 REFERENCES.
927 Albino F, Pinel V, Sigmundsson F (2010) Influence of surface load variations on eruption likelihood:
928 application to two Icelandic subglacial volcanoes, Grímsvötn and Katla. Geophys J Int
929 181:1510–1524. https://doi: 10.1111/j.1365-246X.2010.04603.x
930 Alho P (2003): Land cover characteristics in NE Iceland with special reference to jökulhlaup
931 geomorphology. Geogr Ann A (3–4): 213–227.
932 Alho P, Roberts M, Käyhkö J (2007) Estimating the inundation area of a massive, hypothetical
933 jökulhlaup from northwest Vatnajökull, Iceland. Natural Haz 41: 21-42.
934 Andrés N, Palacios D, Tanarro LM, Fernández JM (2016) The origin of glacial alpine landscape in
935 Tröllaskagi peninsula (North Iceland). Cuadernos Invest. Geogr 42(2), 341–368.
936 https://doi.org/10.18172/ cig.2935
937 Andrès N, Palacios D, Sæmundsson Þ, Brynjólfsson S, Fernández-Fernández JM (2019) The rapid
938 deglaciation of the Skagafjörður fjord, northern Iceland. Boreas 48: 92–106.
939 https://doi.org/10.1111/bor.12341. ISSN 0300-9483.
940 Andresen CS, Bjorck S, Bennike O, HeinemeierJ, Kromer B (2000) What do $\Delta^{14}C$ changes across the
941 Gerzensee oscillation/GI-1b event imply for deglacial oscillations J.Quat Sci , 15: 203–214.

942 Andrews JT, Geirsdóttir Á, Principato S, Kristjánsdóttir GB, Helgadóttir G, Hardardóttir J, Grönvold K,
943 Sveinbjörnsdóttir Á, Drexler J (2002) Distribution, age and geochemistry of the Saksunarvatn
944 10.18 ± cal ka) ash in marine, lake, and terrestrial sediments, NW Iceland. J Quat Sci 17 (8),
945 731-745.
946 Baker, V.R. 1973. Palaeohydrology and sedimentology of Lake Missoula flooding in eastern
947 Washington. Geol Soc Am.. Spec Paper, 144: 1-79.
948 Baynes ERC, Attal Ml, Niedermann S, Kirstein LA, Dugmore AJ, Naylor M (2015) Erosion during
949 extreme flood events dominates Holocene canyon evolution in northeast Iceland PNAS, 112:
950 2355–2360.
951 Benediktsson ÍÖ, Schomacker A, Johnson MD, Geiger AJ, Ingólfsson Ó, Guðmundsdóttir ER (2015)
952 Architecture and structural evolution of an early Little Ice Age terminal moraine at the surge-
953 type glacier Múlajökull, Iceland, J Geophys Res, Earth Surf., 120, 1895–1910.
954 https://doi.org:10.1002/2015JF003514.
955 Benediktsson ÍÖ (2012) Polyphase structural evolution of a fine-grained, fold-dominated end moraine,
956 Brúarjökull surge-type glacier, Iceland. Jökull, 62: 167-183.
957 Benn DI, Evans DJA (2011) Glaciers and Glaciation, Second edition. Hodder Education, London.
958 Benn DI, Fowler AC, Hewitt I, Sevestre H (2019); A general theory of glacier surges. J Glaciology 65,
959 (253), 701-716. https://doi:10.1017/jog.2019.62
960 Birks H, Gulliksen S, Haflidalson H, Mangerud J et al. (1996) New Radiocarbon Dates for the Vedde
961 Ash and the Saksunarvatn Ash from Western Norway. Quaternary Res 45:119–127.
962 Björck S, Rundgren M, Ingólfsson O, Funder S (1997) The Preboreal oscillation around the Nordic
963 Seas: terrestrial and lacustrine responses. Quaternary Sci 12: 455–465.
964 Björnsson H (2017) The Glacier of Iceland, Translation of “Jöklar á Íslandi”. 2009, Atlantis Press,
965 Advances in Quaternary Sci.
966 Björnsson, H., 2002: Subglacial lakes and jökulhlaups in Iceland. Glob Planet Change, 35, 255–271.
967 Björnsson H (1998). Hydrological characteristics of the drainage system beneath a surging glacier.
968 Nature, 395: 771–774.
969 Björnsson H (1992) Jökulhlaups in Iceland: prediction, characteristics and simulation. Ann. Glaciol.,
970 16:95–106.

971 Björnsson H (1974) Explanation of jökulhlaups from Grímsvötn,Vatnajökull, Iceland. Jökull, 24: 1–25.
972 Björnsson H., Pálsson, F, Sigurđsson, O., Flowers, GE (2003) Surges of glaciers in Iceland. Ann.
973 Glaciology, 36: 82-90.
974 Bond GG., Kromer B, Beer J, Muscheler R, Evans M, Showers W. Hoffmann S. Lotti-Bond R, Hajdas
975 I, Bonani G (2001) Persistent Solar influence on North Atlantic climate during the Holocene.
976 Science, 294: 2130–2136.
977 Bos JAA, van Geel B, van der Plicht J, Bohncke SJP (2007) Preboreal climate oscillations in Europe:
978 Wiggle-match dating and synthesis of Dutch high-resolution multi-proxy records. Quat Sci
979 Rev, 26: 1927-1950.
980 Boulton GS, van der Meer JJM, Beets DJ, Hart J, Ruegg GH (1999) The sedimentary and structural
981 evolution of a recent Push moraine complex: Ὀstrømbreen, Spitsbergen. Quat Sci Rev 18:
982 339–371.
983 Brader MD, Lloyd JM, Bentley MJ, Newton AJ (2015) Lateglacial to Holocene relative sea-level
984 changes in the Stykkisholmur area, northern Snæfellsnes, Iceland.J Quat Sci., 30: 497–507.
985 Bronk RC, Albert PG, Blockley SPE, Hardiman M, Housley RA, Lane CS et al. (2015) Improved age
986 estimates for key Late Quaternary European tephra horizons in the RESET lattice. Quat Sci
987 Rev 118:18-32. https://doi.org/10.1016/j.quascirev.2014.11.007
988 Carling PA (2013) Fresh water megaflood sedimentation: what can we learn about generic processes.
989 Earth Sci. Rev125: 87-113.
990 Carrivick JL (2007). Hydrodynamics and geomorphic work of jökulhlaups (glacial outburst floods) from
991 Kverkfjöll volcano, Iceland. Hydrol Process 21: 725–740.
992 Carrivick JL, Tweed FS., Carling PA, Alho P, Marren PM, Staines K, Russell AJ, Rushmer EL, Duller R
993 (2013) Discussion of field evidence and hydraulic modelling of a large Holocene jökulhlaup at
994 Jökulsá á Fjöllum channel, Iceland' by Douglas Howard, Sheryl Luzzadder-Beach and Timothy
995 Beach, 2012, Geomorphology, 201, 512-519
996 Carrivick JL, Russell AJ, Rushmer EL, Tweed FS, Marren PM, Deeming KR, Lowe HG (2009)
997 Geomorphological evidence towards a de-glacial control on volcanism. Earth Surface. Process
998 Landf 34: 1164–1178.
999 Clague JJ, Barendregt R; Enkin RJ, Foit FF (2003) Paleomagnetic and tephra evidence for tens of
1000 Missoula floods in southern Washington. Geology Geol Soc. Am 31: 247–250.

1001 Condron A, Winsor P (2012). Meltwater routing and the Younger Dryas. Proc Natl Acad Sci U S.,
1002 109:19928–19933. https://doi:10.1073/pnas.1207381109.
1003 Dahl-Jensen D. and NEEM community members (2013) Eemian interglacial reconstructed from a
1004 Greenland folded ice core. Nature, 493. 489–49.
1005 Dahl SO, Nesje A, Lie O, Fjordheim K, Matthews JA (2002) Timing, equilibrium-line altitudes and
1006 climatic implications of two early-Holocene glacier readvances during the Erdalen Event at
1007 Jostedalsbreen, western Norway. Holocene 12:17–25.
1008 Doyle S, Hubbard A, van de Wal R, Box J, van As D, Scharrer K, Meierbachtol T, Smeets, P, et al.
1009 (2015) Amplified melt and flow of the Greenland ice sheet driven by late-summer cyclonic
1010 rainfall. Nature Geo. 10.1038/NGEO2482.
1011 Eason D, Sinton JM, Grönvold K., Kurz M (2015) Effects of deglaciation on the petrology and eruptive
1012 history of the Western Volcanic Zone, Iceland. B Volcanol 77: 47. https://doi10.1007/s00445-
1013 015-0916-0
1014 Eiríksson J, Knudsen KL, Haflidason H, Henriksen P (2000) Late-glacial and Holocene
1015 palaeoceanography of the North Icelandic shelf. J Quat Sci 15, 23–42.
1016 Eksinchol I, Rudge JF, Maclennan J (2019) Rate of melt ascent beneath Iceland from the magmatic
1017 response to deglaciation. Geochem Geophy Geosy 20: 2585-2605.
1018 Elíasson S (1977) Molar um Jökulsarhlaup og Asbyrgi. Natturufæjingurinn 47, 160–179.
1019 Eyles N, Boyce JI, Barendregt RW (1999) .Hummocky moraine: Sedimentary record of stagnant
1020 Laurentide Ice Sheet lobes resting on soft beds. Sediment Geol 123: 163–174.
1021 Https://doi.org:10.1016/S0037-0738(98)00129-8
1022 Etzelmüller B, Farbrot H, Guðmundsson Á, Humlum O, Tveito O., Björnsson H (2007). The regional
1023 distribution of mountain permafrost in Iceland. Permafrost Periglac 18: 185-199.
1024 Fard AM (2002) Large dead-ice depressions in flat-topped eskers: evidence of a Preboreal jökulhlaup
1025 in the Stockholm area, Sweden. Glob Planet Change 35, 273–295
1026 Fitzpatrick AAW., Hubbard AL, Box JE, Quincey DJ, van As D, Mikkelsen APB, Doyle SH, Dow CF,
1027 Hasholt B, Jones GA (2014) A decade (2002–2012) of supraglacial lake volume estimates
1028 across Russell Glacier, West Greenland. Cryosphere, 8, 107-121, https://doi.org/10.5194/tc-8-
1029 107-2014, 2014.

1030 Flowers GE, Björnsson H, Pálsson F (2003) New insights into the subglacial and periglacial hydrology
1031 of Vatnajökull, Iceland, from a distributed physical model. J Glaciology, 49, 165,257-270.
1032 GAPHAZ (2017) Assessment of Glacier and Permafrost Hazards in Mountain Regions – Technical
1033 Guidance Document. Prepared by Allen, S., Frey, H., Huggel, C. et al. Standing Group on
1034 Glacier and Permafrost Hazards in Mountains (GAPHAZ) of the IACS and IPA. Zurich,
1035 Switzerland / Lima, Peru.
1036 Geirsdóttir Á, Eiríksson J (1996) A review of studies of the earliest glaciations in Iceland.Terra Nova 8:
1037 400-414.
1038 Geirsdóttir Á, Hardardóttir J, Sveinbjörnsdóttir ÁE (2000) Glacial extent and catastrophic meltwater
1039 events during the deglaciation of Southern Iceland .Quat Sci Rev 19: 1749-1761.
1040 Geirsdóttir A., Miller GH, Axford Y, Olafsdóttir S (2009) Holocene and latest Pleistocene climate and
1041 glacier fluctuations in Iceland. Quat Sci.Rev 28 (21-22): 2107-2118.
1042 Geirsdóttir Á, Miller GH, Larsen GJ, Ólafsdótti S (2013) Abrupt Holocene climate transitions in the
1043 northern North Atlantic region recorded by synchronized lacustrine records in Iceland. Quat
1044 Sci Rev 70 (15): 48-62.
1045 Goslar T, Arnold M, Tisnerat-Laborde N, Czernik J, Wieckowski K (2000) Variations of Younger Dryas
1046 atmospheric radiocarbon explicable without ocean circulation changes. Nature 403: 877–880.
1047 Grönvold K, Oskarsson N, Johnsen SJ, Clausen HB, Hammer CU, Bond G, Bard E (1995) Ash layers
1048 from Iceland in the Greenland GRIP ice core correlated with oceanic and land based
1049 sediments. Earth Planet Sci Lett 135, 149-155.
1050 Guðmundsdóttir ER, Larsen GD, Björck S, Ingólfsson Ó, Striberger J (2016) A new high-resolution
1051 Holocene tephra stratigraphy in eastern Iceland: Improving the Icelandic and North Atlantic
1052 tephrochronology. Quat Sci Rev 150, 234-249. https://doi: 10.1016/j.quascirev.2016.08.011
1053 Guðmundsdóttir ER, Larsen GD, Eiríksson J (2012) Tephra stratigraphy on the North Icelandic shelf:
1054 extending tephrochronology into marine sediments off North Iceland. Boreas, 41: 718-734.
1055 Guðmundsson Á (2000) Frerafjöll, Urðarbingir á Tröllaskaga. MSc thesis, University of Iceland,
1056 Reykjavik, Iceland.
1057 Guðmundsson MT, Sigmundsson F, Björnsson.H (1997) Ice – volcano interaction of the 1996 Gjálp
1058 subglacial eruption, Vatnajökull, Iceland.Nature,389(6654): 954-957.
1059

1060 Guðmundsson MT, Björnsson H, Pálsson F (1995) Changes in jökulhlaup sizes in Grímsvötn,
1061 Vatnajökull, Iceland, 1934-91, deduced from in-situ measurements of subglacial lake volume.
1062 J.Glaciology, 41 (38): 263-272.
1063 Gylfadóttir SS, ÞórarinsdóttirT, Pagneux E, Björnsson BB (2017) Hermun jökulhlaupa í Jökulsá á
1064 Fjöllum með GeoClaw. Icelandic Meteorologic Office, VÍ 2017-004, ISSN 1670-8261.
1065 Haflidason H, Eiríksson J, Van Kreveld S (2000) The tephrochronology of Iceland and the North
1066 Atlantic region during the Middle and Late Quaternary: a review. J Quat Sci 15:3–22.
1067 Halldórsson SA, Oskarsson N, Grönvold K, Sigurdsson G, Sverrisdóttir G, Steinthorsson S (2008)
1068 Isotopic heterogeneity of the Thjorsa lava – implications for mantle sources and crustal
1069 processes within the Eastern Rift Zone, Iceland. Chem Geol, 255, 1-3: 305–316.
1070 Harning DJ, Geirsdóttir Á, Miller GH, Zalzal K (2016). Early Holocene deglaciation of Drangajökull,
1071 Vestfirðir, Iceland. Quat Sci Rev 153:192-198.
1072 Hartley ME, ThordarsonT, de Joux A (2016) Postglacial eruptive history of the Askja region, North
1073 IcelandBull Volcanol 78: 28. https://doi.org/10.1007/s00445-016-1022-7.
1074 Hjartardóttir ÁR, Einarsson P (2017) Eru Hljóðaklettar og Rauðhólar í Jökulsárgljúfrum gervigígar?
1075 Haustráðstefna Jarðfræðafélags Íslands 17: 7-8.
1076 Hjartarson Á (2003) The Skagafjörður unconformity, north Iceland, and its geological history. PhD
1077 thesis, Geol. Museum, Univ Copenhagen.
1078 Hoskuldsson A, Sparks RSJ, Carroll MR (2006) Constraints on the dynamics of subglacial basalt
1079 eruptions from geological and geochemical observations at Kverkfjoll, E Iceland. B Volcanol
1080 68: 689–701. https://doi 10.1007/s00445-005-004 3-4.
1081 ICS 2018. International commission for Stratigraphy - International chronostratigraphic chart v2018/07.
1082 http://www.stratigraphy.org/
1083 Jennings A, Syvitski J, Gerson L, Grönvold K, Geirsdóttir Á, Hardardóttir J, Andrews J, Hagen S
1084 (2000) Chronology and paleoenvironments during the Late Weichselian deglaciation of the
1085 Southwest Iceland Shelf. Boreas 29: 167–183.
1086 Jóhannsdóttir GE (2007) Mid-Holocene to late glacial tephrochronology in west Iceland as revealed in
1087 three lacustrine environments. MS thesis, Univ Iceland, Reykjavík.
1088 Jonásson K (1994) Rhyolite volcanism in the Krafla central volcano, north-east Iceland. B Volcanol.
1089 56:516-528.

1090 Jones G, Davies S, Farr G, Bevan J (2017) Identification of the Askja-S Tephra in a rare turlough
1091 record from Pant-y-Llyn, south Wales. Proc Geologists' Assoc 128 (4), 523-530.
1092 http://dx.doi.org/10.1016/j.pgeola.2017.05.010
1093 Jull M, McKenzie D (1996) The effect of deglaciation on mantle melting beneath Iceland. J Geophys
1094 Res. 107: 21815–21828.
1095 Kaldal I, Víkingsson S (1990) Early Holocene deglaciation in central Iceland. Jökull, 40, 51–66.
1096 Kaldal I, Víkingsson S (2000). Jarðgrunnskort af Eyjabökkum. Orkustofnun report OS-2000/068.
1097 (Reykjavík, Iceland, 10 p.).
1098 Kirkbride, M.P., Dugmore, A.J., Brazier, V. 2006. Radiocarbon dating of mid-Holocene megaflood
1099 deposits in the Jökulsá á Fjöllum, north Iceland. Holocene, 16 (4), 605-609.
1100 Knudsen O (1995) Concertina eskers, Brúarjökull, Iceland: An indicator of surge-type glacier
1101 behaviour, December 1995. Quat Sci Rev 14:487-493. https://doi.org10.1016/0277-
1102 3791(95)00018-K.
1103 Knudsen O, Marren PM 2002. Sedimentation in a volcanically dammed valley, Brúarjökull, Quat Sci
1104 Rev 21:1677–1692. https://doi10.1016/S0277-3791(01)00144-5.
1105 Klingbjer P (2004) Recurring Jökulhlaups in Sälka, Northern Sweden. Geogr Ann A. Physic.Geogr, 86
1106 (2), 169-179.
1107 Kobashi T, Menviel L, Jeltsch-Thömmes A, Vinther BM, Box JE, Muscheler R., et al. (2017) Volcanic
1108 influence on centennial to millennial Holocene Greenland temperature change. Nature,
1109 Scient.Rep 7, 1441. https://doi.org: 10.1038/s41598-017-01451-7.
1110 Koren H, Svendsen JI, Mangerud J, Furnes H (2008) The Dimna Ash — a 12.8 14C ka-old volcanic
1111 ash in Western Norway. Quat Sci Rev, 27: 85–94.
1112 Lacasse C, Carey S, Sigurdsson H (1998) Volcanogenic sedimentation in the Iceland Basin: influence
1113 of subaerial and subglacial eruptions J Volcanol Geotherm Res 83: 47–73.
1114 Langdon PG, Leng MJ, Holmes N, Caseldine CJ (2010) Lacustrine evidence of early-Holocene
1115 environmental change in northern Iceland: a multiproxy palaeoecologyand stable isotope
1116 study. Holocene 20: 205–214.
1117 Larsen DJ, Mille GH, Geirsdóttir A, Olafsdóttir S (2012) Non-linear Holocene climate evolution in the
1118 North Atlantic: a high-resolution, multi-proxy record of glacier activity and environmental
1119 change from Hvítarvatn, central Iceland. Quat Sci. Rev 39: 14-25.

1120 Larsen G, Eiríksson J (2007) Late Quaternary terrestrial tephrochronology of Iceland, frequency of
1121 explosive eruptions, type and volume of tephra deposits. J Quat Sci, 23:109–120.
1122 https://doi.org/10.1002/jqs.1129
1123 Larsen G, Eiríksson J, Knudsen KL, Heinemeier J (2002) Correlation of late Holocene terrestrial and
1124 marine tephra markers in North Iceland. Implications for reservoir age changes and linking
1125 land-sea chronologies in the northern North Atlantic. Polar Res 21, 283-290.
1126 Le Breton E, Dauteuil O, Biessy G (2010) Post-glacial rebound of Iceland during the Holocene. J Geol
1127 Soc., London, 167, 417–432. https://doi.org: 10.1144/0016-76492008-126.417.
1128 Licciardi JM, Kurz MD, Curtice JM (2007) Glacial and volcanic history of Icelandic table -mountains
1129 from cosmogenic ^{3}He exposure ages. Quat Sci Rev 6:1529–1546. https://doi.org
1130 10.1016/j.epsl.2006.03.016
1131 Lind E, Wastegård S (2011) Tephra horizons contemporary with short early Holocene climate
1132 fluctuations: New results from the Faroe Islands. Quaternary Intern, 246: 157-167.
1133 Lønne I (2016) A new concept for glacial geological investigations of surges, based on High-Arctic
1134 examples (Svalbard), Quat Sci Rev 132: 74-100. https://doi:
1135 10.1016/j.quascirev.2015.11.0090.
1136 Maclennan J, Jull M, McKenzie D, Slater L, Grönvold K (2002) The link between volcanism and
1137 deglaciation in Iceland. Geochem Geophy Geosy 3, 1062. https://doi:10.1029/2001GC000282
1138 Maizels J (1997) Jökulhlaup deposits in proglacial areas. Quat Sci Rev 16:793–819.
1139 Maizels J (1991) The origin and evolution of Holocene sandur deposits in areas of jökulhlaup
1140 drainage, Iceland. In: Maizels J, Caseldine C, Eds., Environmental Change in Iceland: Past
1141 and Present. Kluwer Academic Publ , Dordrecht, 267–279.
1142 Maizels JK, Russell AJ (1992) Quaternary perspectives on jökulhlaup prediction, in Gray, J. M. (ed.)
1143 Applications of Quaternary Research, Quaternary Proceed, 2: 133-153.
1144 Mangerud J, Furnes H, Johansen J (1986). A 9000 year ash bed on the Faroe Islands. Quaternary
1145 Res.26, 262–265.
1146 Matero SO, Gregoire LJ, Ivanovic RF, Tindall JC, Haywood AM (2017) The 8.2 ka cooling event
1147 caused by Laurentide ice saddle collapse. Earth Planet Sci Lett 473: 205-214.
1148 https://doi.org/10.1016/j.epsl.2017.06.011

1149 Matthews JA, Shakesby RA, Schnabel C, Freeman S (2008) Cosmogenic ^{10}Be and ^{26}Al ages of
1150 Holocene moraines in southern Norway I: testing the method and confirmation of the date of
1151 the Erdalen Event (c. 10 ka) at its type-site. Holocene, 18:1155-1164.
1152 https://doi.org.org/10.1177/0959683608096585

1153 Meier MF, Post AS (1969) What are glacier surges? Can.J Earth Sci. 6, 807-817.

1154 Mikkelsen AB, Hubbard A, MacFerrin M, Box JE, Doyle S, Fitzpatrick A., Hasholt B, Bailey HL,
1155 Lindbäck K, Pettersson R (2016) Extraordinary runoff from the Greenland ice sheet in 2012
1156 amplified by hypsometry and depleted firn retention. Cryosphere 10, 1147-1159.

1157 Möller R, Möller M, Björnsson H., Guðmundsson S, Pálsson F, Oddsson B, Kukla P. Schneider C
1158 (2013) MODIS-derived albedo changes of Vatnajökull (Iceland) due to tephra deposition from
1159 the 2004 Grímsvötn eruption. Int J Appl Earth Obs 2:, 256–269.

1160 Norðdahl H, Ingólfsson O, Vogler ED, Steingrímsson BO, Hjartarson Á (2019) Glacio-isostatic age
1161 modelling and Late Weichselian deglaciation of the Lögurinn basin, East Iceland. Boreas, 41:
1162 563-580. https://doi.org/10.1111/bor.12366

1163 NGRIP members (2004) High-resolution record of Northern Hemisphere climate extending into the last
1164 interglacial period. Nature 431: 147-151.

1165 Óladóttir BA, Sigmarsson O, Larsen G, Devidal J-L (2011a) Provenance of basaltic tephras from
1166 Vatnajökull subglacial volcanoes, Iceland as determined by major- and trace-element
1167 analyses. Holocene, 21: 1037–1048.

1168 Óladóttir BA, Larsen G, Sigmarsson O (2011b) Holocene volcanic activity at Grímsvötn, Bárdarbunga
1169 and Kverkfjöll subglacial centres beneath Vatnajökull, Iceland. B Volcanol, 7: 1187-1208

1170 Olszewski A, Weckwerth P (1999) The morphogenesis of kettles in the Höfðabrekkujökull forefield,
1171 Mýrdalssandur, Iceland, Jökull, 47: 71 88.

1172 Ott F, Wulf S, Serb J, Słowiński M, Obremska M, Tjallingii R, Błaszkiewicz M, Brauer A (2016)
1173 Constraining the time span between the Early Holocene Hässeldalen and Askja-S Tephras
1174 through varve counting in the Lake Czechowskie sediment record, Poland. J Quat Sci 31:103-
1175 113https://doi.org/10.1002/jqs.2844

1176 Pagli C, Sigmundsson F, Pedersen R, Einarsson P, Arnadóttir T, Feigl KL (2007) Crustal deformation
1177 associated with the 1996 Gjalp subglacial eruption, Iceland: InSAR studies in affected areas
1178 adjacent to the Vatnajökull ice cap. Earth Planet Sci Lett 259: 24–33.

1179 Pagli C, Sigmundsson F (2008) Will present day glacier retreat increase volcanic activity? Stress
1180 induced by recent glacier retreat and its effect on magmatism at the Vatnajökull ice cap,
1181 Iceland. Geophys Res Lett 35: L09304.
1182 Patton H., Hubbard A., Bradwell, T., Schomacker A. 2017. The configuration, sensitivity and rapid
1183 retreat of the Late Weichselian Icelandic ice sheet. Earth Sci Rev 166: 223-245.
1184 Rasmussen SO, Andersen KK, Svensson AM, Steffensen JP., Vinther, B, Clausen HB et al. (2006) A
1185 new Greenland ice core chronology for the last glacial termination. J.Geophys Res.111, 1-15.
1186 Rasmussen TL, Wastegard S, Kuijpers A, van Weering TCE, Heinemeier J, Thomsen E (2003)
1187 Stratigraphy and distribution of tephra layers in marine sediment cores from the Faroe Islands,
1188 North Atlantic. Marine Geol. 199, 263–277.
1189 Rasmussen TL, Thomsen E, Nielsen T, Wastegård S (2011) Atlantic surface water inflow to the Nordic
1190 seas during the Pleistocene–Holocene transition (mid–late Younger Dryas and Pre-Boreal
1191 periods, 12 450–10 000 a BP) J. Quat Sci. 26: 723–733,
1192 Rasmussen SO, Bigler M, Blockley SP, Blunier T, Buchardt SL, Clausen HB., et al. (2014)
1193 Stratigraphic framework for abrupt climatic changes during the Last Glacial period based on
1194 three synchronized Greenland ice-core records: Refining and extending the INTIMATE event
1195 stratigraphy. Quat Sci Rev 106:14-28.
1196 Roberts MJ, Russell AJ, Tweed FS, Knudsen Ó (2000) Ice fracturing during Jokulhlaups: Implications
1197 for englacial floodwater routing and outlet development. Earth Surf Process Landf 25: 1429-
1198 1446. Https://doi.org10.1002/1096-9837(200012)25.
1199 Roberts MJ, Tweed FS, Russell AJ, Knudsen O, Harris TD (2003) Hydrologic and geomorphic effects
1200 of temporary ice dammed lake formation during jökulhlaups. Earth Surf Process Landf 28:
1201 723–737.
1202 Rudoy AN, Baker VR (1993) Sedimentary effects of cataclysmic late Pleistocene glacial outburst
1203 flooding, Altay Mountains, Siberia. Sediment Geol. 85: 53-62.
1204 Rushmer EL (2006) Sedimentological and geomorphological impacts of the jökulhlaup (glacial outburst
1205 flood) in January 2002 at Kverkfjöll, northern Iceland. Geogr Ann A:1–11.
1206 Russell AJ (1993) Supraglacial lake drainage near Søndre Strømfjord, Greenland. J Glaciology 39:
1207 431–433

1208 Russell AJ, Knight PG, Van Dijk TAGP (2001) Glacier surging as a control on the development of
1209 proglacial, fluvial landforms and deposits, Skeidararsandur, Iceland. Glob Planet Change
1210 28:163–174..
1211 Russell AJ, Knudsen Ó (1999) An ice-contact rhythmite (turbidite) succession deposited during the
1212 November 1996 catastrophic outburst flood (jökulhlaup), Skeiðarárjökull, Iceland. Sediment
1213 Geol 127(1-2): 1-10.
1214 Russell AJ, Marren PM (1998). Younger Dryas (Loch Lomond Stadial) jökulhlaup deposits, Fort
1215 Augustus, Scotland. Boreas 27: 231–242.
1216 Russell AJ, Tweed FS, Knudsen O, Roberts MJ., Harris TD, Marren PM (2002) Impact of the July
1217 1999 jökulhlaup on the proximal river Jökulsa a Solheimasandi, Myrdalsjökull glacier, southern
1218 Iceland. IAHS Publ. Nr 271, Reykjavik: 249–254.
1219 Sæmundsson K.(1991) Geology of the Krafla system. In: Gardarsson A, Einarsson A (editors) Nfitttira
1220 Myvatns. Hid Islenska Nattirufraedif 61ag, Reykjav N: 25-95.
1221 Sæmundsson K. (1973) Straumraðkajar klappir ı´ kringum Asbyrgi.Natturufæjingurinn 43: 52–60.
1222 Sæmundsson K, Hjartarson Á, Kaldal I, Sigurgeirsson MÁ., Kristinsson SG, Víkingsson S (2012)
1223 Geological Map of the Northern Volcanic Zone, Iceland. Northern Part. 1:100,000 (Iceland
1224 GeoSurvey, Reykjavik, Iceland).
1225 Schomacker A, Benediktsson IO, Ingólfsson O (2014) The Eyjabakkajökull glacial landsystem,
1226 Iceland: Geomorphic impact of multiple surges Geomorphology, 218, 98–107. Https://doi.org:
1227 10.1016/j.geomorph.2013.07.005
1228 Sharp M, (1985) Sedimentation and stratigraphy at Eyjabakkajökull — an Icelandic surging glacier.
1229 Quaternary Res 24: 268–284.
1230 Sigurðsson H. and Sparks RSJ (1978) Rifting episode in North Iceland in 1874–1875 and the
1231 eruptions of Askja and Sveinagjá. B Volcanol 41. 149–167.
1232 Sigurgeirsson, M. Á., 2016. Eldar í Öskjukerfi fyrir um 11 þúsund árum (Volcanic episode in the Askja
1233 volcanic system 11.000 years ago), Náttúrufræðingurinn, 86 (3-4), 76-90.
1234 Sigurgeirsson MÁ., Hjartarson Á., Kaldal I, Sæmundsson K, Kristinsson GS, Víkingsson S (2015)
1235 Geological Map of the Northern Volcanic Zone, Iceland. Southern Part. 1:100 000. Reykjavík:
1236 Iceland GeoSurvey.

1237 Sinton J, Grönvold K, Sæmundsson K (2005) Postglacial eruptive history of the Western Volcanic
1238 Zone, Iceland. Geochem Geophy Geosy 6,12. https://doi.org/10.1029/2005GC001021
1239 Slater L, Jull M, McKenzie D, Grönvold K (1998). Deglaciation effects on mantle melting under Iceland:
1240 Results from the northern volcanic zone. Earth Planet. Sci Letters Lett. 164:151–154.
1241 Smellie JL (2008) Basaltic subglacial sheet-like sequences: evidence for two types with different
1242 implications for the inferred thickness of associated ice. Earth Sci Rev 88: 60–88.
1243 Snorrason A, Jónsson P, Pálsson S, Àrnason S, Sigurðsson O, Vikingsson S, Sigurðsson À,
1244 Zóphóniasson S (1997) The jökulhlaup in Skeiðarársandur in the fall of 1996—extent of
1245 inundation, discharge and sediment transport) (in Icelandic). In: Vatnajökull—Gos og Hlaup
1246 1996 (Vatnajökull eruption and jökulhlaup 1996) (ed. by II. Haraldsson), 79-137. The Icelandic
1247 Public Road Admin., Reykjavik, Iceland.
1248 Striberger S, Björck S, Holmgren L, Hamerlik L (2012) The sediments of Lake Lögurinn – a unique
1249 proxy record of Holocene glacial meltwater variability in eastern Iceland. Quat Sci Rev 38: 76-
1250 88.
1251 Striberge J, Björck S, Benediktsson ÍÖ., Snowball I, Uvo CB, Ingólfsson Ó, Kjær KH (2011) Climatic
1252 control of the surge periodicity of an Icelandic outlet glacier. J Quat Sci 26: 561–565.
1253 Stuiver M, Reimer PJ, Braziunas TF. (1998) High-precision radiocarbon age calibration for terrestrial
1254 and marine samples. Radiocarbon, 40, 3: 1127-1151]
1255 Stuiver M, Braziunas TF (1989) Atmospheric 14C and Century-Scale Solar Oscillations. Nature, 338,
1256 1041-1083. http://dx.Doi.org/10.1038/338405a0
1257 Sund M, Eiken T, Hagen JO, Kääb A (2009) Svalbard surge dynamics derived from geometric
1258 changes. Ann Glaciol 50 (52): 50-60.
1259 Thorarinsson S (1969) Glacier surges in Iceland with special reference to the surges of Bruarjokull.
1260 Can J Earth Sci, 6(4), Part 2: 875–882.
1261 Thordarson T (2014) The widespread ~10ka Saksunarvatn tephra is not a product single eruption
1262 American Geophysical Union, Fall Meeting 2014, abstract V24B-04612.
1263 Tómasson H (1973) Hamfarahlaup i Jökulsá a Fjöllum. Náttúrufraiding urinn 43: 12–34.
1264 Tweed FS (2000). Jökulhlaup initiation by ice-dam flotation: the significance of glacier debris content.
1265 Earth Surf Process Landf 25: 105–108.

1266 Van Vliet-Lanoë B, Bergerat F, Allemand P, Innocent C, Guillou H, Cavailhes T, Guðmundsson Á,
1267 Chazot G, Schneider JL, Grandjean P, Liorzou C, Passot S (2019) Tectonism and volcanism
1268 enhanced by deglaciation events in southern Iceland. Quaternary Res
1269 https://doi.org/10.1017/qua.2019.68.
1270 Van Vliet-Lanoë B, Schneider JL, Guðmundsson Á, Guillou H, Nomade S, Chazot G, Liorziou C,
1271 Guégan S (2018) Eemian estuarine record forced by glacio-isostasy (S Iceland) - link with
1272 Greenland and deep sea records. Can J Earth Sc 55 (2): 154-171. Https:// 10.1139/cjes-2017-
1273 0126.
1274 Van Vliet-Lanoë B, Pissart A, Baize S, Brulhet J, Ego E (2019) Evidence of multiple thermokarst
1275 events in northeastern France and southern Belgium during the two last glaciations. A
1276 discussion on 'Features caused by ground ice growth and decay in Late Pleistocene fluvial
1277 deposits, Paris basin, France' (Bertran et al. 2018). Geomorphology 327: 613-628.
1278 https://doi.org: GEOMOR-06499.
1279 Van Vliet-Lanoë B, Guðmundsson Á, Guillou H, Duncan RA, Genty D, Ghaleb B, Gouy S, Récourt P,
1280 Scaillet S (2007) Limited glaciation and very early deglaciation in central Iceland: Implications
1281 for climate change. CR Geoscience, 339, 1-12.
1282 Van Vliet-Lanoë B, Bourgeois O, Dauteuil O, Embry JC, Guillou H, Schneider JL (2005) Deglaciation
1283 and volcano-seismic activity in Northern Iceland: Holocene and Early Eemian (The Syðra
1284 Formation). Geodin Acta 18: 81–100.
1285 Van Vliet-Lanoë B, Guðmundsson Á, Guillou H, van Loon AJ, De Vleeschouwer F (2010) Glacial
1286 Terminations II and I as recorded in NE Iceland. Geologos 16: 201–223.
1287 Van Vliet-Lanoë B, Van Cauwenberge AS, Bourgeois O., Dauteuil O, Schneider JL (2001) A candidate
1288 for The Last Interglacial record in northern Iceland: the Syðra Formation. Stratigraphy and
1289 sedimentology. C R Geoscience, 332:577–584.
1290 Voelker AHL, Haflidason H (2015) Refining the Icelandic tephrachronology of the last glacial period –
1291 The deep-sea core PS2644 record from the southern Greenland Sea. Glob Planet Change
1292 131: 35–62.
1293 Vogfjörd KS, Jakobsdóttir SS, Guðmundsson GB, Roberts MJ, Agustsson K, Arason T, et al. (2005)
1294 Forecasting and monitoring a subglacial eruption in Iceland. EOS 86:245-248.

1295 Vonmoos M, Beer J, Muscheler R (2006) Large variations in Holocene solar activity: Constraints from
1296 10Be in the Greenland Ice Core Project ice core. J Geoph Res 111: A10105. Https://doi.org:
1297 10.1029/2005JA011500.
1298 Waitt RB (2002). Great Holocene floods along Jökulsá á Fjöllum, north Iceland. In: Martini P.I., Baker
1299 V.R., Garzón G. (Eds.), Flood and Megaflood Processes and Deposits: Recent and Ancient
1300 Examples. Spec Publ Int Ass Sedimentol 32, 37–51.
1301 Waitt RB (1985) Case for periodic, colossal jökulhlaups from Pleistocene glacial Lake Missoula. Geol
1302 Soc Am Bull. 96 (10): 1271–1286.
1303 Waller RI, Murton JB, Kristensen L (2012) Glacier-permafrost interactions: Processes, products and
1304 glaciological implications. Sed Geol 255–256:1–28. https://Doi:
1305 10.1016/j.sedgeo.2012.02.005
1306 Wohlfarth B, Blaauw M, Daviess SM, Andersson M, Wastegård S, Hormes A, Possnert G (2006)
1307 Constraining the age of Lateglacial and early Holocene pollen zones and tephra horizons in
1308 southern Sweden with Bayesian probability methods. J Quarternary Sci 21: 321–334.
1309 https://doi.org:10.1002/jqs.996.
1310 Wylie J, Voight B, Whitehead J (2000). Instability of magma flow from volatile-dependant viscosity.
1311 Science 285: 1883-1885.
1312
1313 **FIGURES CAPTIONS**
1314
1315 Figure 1: A) Early Holocene jökulhlaup trajectories mapped with field observations and photographic
1316 interpretation. B) Cartographic illustration of the deglaciation history of Iceland, based on
1317 Kaldal and Víkingsson (1990) and recent geological maps (Sæmundsson et al. 2012;
1318 Sigurgeirsson et al. 2015), complemented by new photographic and/or field observations,
1319 tephrostratigraphy and correlations explained in the text.
1320
1321 Figure 2 Map of the maximal extent (Early Holocene) of floods in A) the Skjálfandafljót and B) the
1322 Jökulsá á Fjöllum Rivers. Light blue corresponds to the mapped largest flood extent, probably

9.9 cal ka. Dark blue corresponds to the Late Holocene jökulhlaup pathways. Present-day glacial limits. Explanations and dating in § 4 Data.

Figure 3: Chronology of the recorded tephra and potential floods in relation to climate, 8–15 ka BP: potential impact of deglaciation induced by climate warming. Arrows – potential jökulhlaup events; SKA – Skjálfandafljöt River; JF – Jökulsá á Fjöllum River; SDJ – Skeiðararjökull Glacier, BRU: Jökulsá á Brú

A) Warming potentially linked to solar activity, derived from $\delta^{14}C$ (Stuiver and Braziunas, 1988). Entire Saksunarvatn Tephra record from the literature shown in grey.

B) Regional mean temperatures from the NGRIP $\delta^{18}O$ isotope curve (NGRIP, 2004). For tephra sources, see Table 1; SAKS – range of the Saksunarvatn event.

Tephra from Grímsvötn Volcano in black; Bárðarbunga Volcano in red; tephra from Askja Volcano in white, other rhyolitic tephra in yellow. The position of glacial advances are shown in blue. PBE–Preboreal cooling event; AL– Alleröd; ACE– Alleröd cooling event; BCE– Bölling cooling event.

Figure 4: map of the largest floods and morainic arc (partly eroded) preserved in the lower Jökulsá á Fjöllum.

Figure 5. Hnausar.(images from Google Earth [GE]). A) Deglaciation paleolake. B) Glacial surge (11.2 cal ka). C) Piercing by jökulhlaup. D) Tephrostratigraphic record.

Figure 6: Evidence of jökulhlaups in the Hólssandur Plateau at 380 m (images GE). A) Large, flat lozenge-shaped hydraulic dune at Kvensöðull. B) Details of the dunes, showing evidence of surface megaripples, and terrace levels from the end of the flood. C) Evidence south of A of a residual terminal moraine and cinder cones, to the west, both eroded by floods, Note s, eroded by floods.

Figure 7: Evidence of terminal moraines on the Jökulsá á Fjöllum and Þjórsá–Tungnaá Rivers. North is upwards. A) Relict of a terminal moraine, SW of the Hrossaborg, eroded by floods – the

Hrossaborg Advance, c. 10.3 cal ka (image Landmælingar Island [LmIs]). B) Terminal moraine that was issued from the Bruarjokul outlet glacier, NE of the Vaðalda – the Kreppa Advance, c. 9.3 cal ka pierced by jökulhlaup (image from LmIs). C) Kisa Advance, c. 9.3 cal ka, overlapped in the east by the Þjórsá Lava (8.7 cal ka; image LmIs). D) Megaripples in basaltic sands (25 m wide) at the SW foot of the Vaðalda Volcano (Sample Dingjuvatn D3; image LmIs). The North is upward.

Figure 8: Paths of the early Holocene jökulhlaup in the Skalfandafljót, Fnjoskadalur and Eyafjörður. Notice the location of disrupted glacial tongue that hypothetically (?) also reached the lower Skalfandafljót, but have been now eroded.

Figure 9: Ljósavatn and Halslón records. A-B) Ljósavatn pitted moraine. Evidence of jökulhlaup deposits, with iceberg kettle hole in juxtaglacial position The final infilling reworks an Askja tephra much older than the Askja S (Askja PB), Stórutjarnaskóli Quarry. B) Loess section above the Preboreal tillite; the Askja PB is involved with the loadcatsing in the grey loess. C-D-E: Upper Hálslón Lake record. C) Deglacial braided sandur, reworking the Askja E Tephra; D) Twinned Saksunarvatn Tephra deposits in juxtaglacial position, deformed by late, but limited, glaciotectonics. E) Undeformed Saksunarvatn Tephra, buried by jökulhlaup deposits and loess in a lateral valley (Van Vliet-Lanoë et al. 2010).

Figure 10: Composite record of main sections, with reference to the main sources of tephra. JL – jökulhlaup deposits, Gl – tillite. Iceberg scours at Varghóll and iceberg thermokarst at Ljósavatn. Classic thermokast (kettle hole) at Palmholt. Sections are located on figures 2-4-9-10.

Figure 11: A, B) Detail of the N moraine of the Eyjabakkajökull Glacier (images LmIs), the thick white arrow indicate 1890 stacked “push” moraines following Schomaker et al. 2014). C) Potential evidence of stacked, permafrosted moraines (Hólssandur). D) Stacked, permafrosted moraine, Usherbreen Glacier, Svalbard (image courtesy of J.O. Hagen).

Figure 12: The South-West A) Esker at Búðarháls, eroded by a jökulhlaup. B–D) Varghóll section, with terminal ridges (thick arrows on C; images LmIs), iceberg scours (B) incising a basaltic tephra deposit containing Vedde Ash pellets (stars), and a tillite stacking pattern (D).

Figure 13: Routes (black) of the early jökulhlaups in relation to the Holocene glacial advances (10.3 ka – white, 9.3 ka – yellow). Potential subglacial lake / aquifers extents are shown in blue, related to a 125 m and 250 m residual glacio-isostatic subsidence. Black stippled line – present-day glaciers, white stippled line – 10.3 cal ka glaciers

Table 1: Chronology of the significant eruptions of Grímsvötn, Bárðarbunga, Askja, Katla and Krafla volcanoes from Late Glacial to 8.2 cal ka.

Table 2: Geochemical analysis of the tephra (ICPMS AES and * microprobe average; Microprobe on Supplement table 1)

Supplement available on

https://static-content.springer.com/esm/art%3A10.1007%2Fs00531-020-01833-9/MediaObjects/531_2020_1833_MOESM1_ESM.pdf

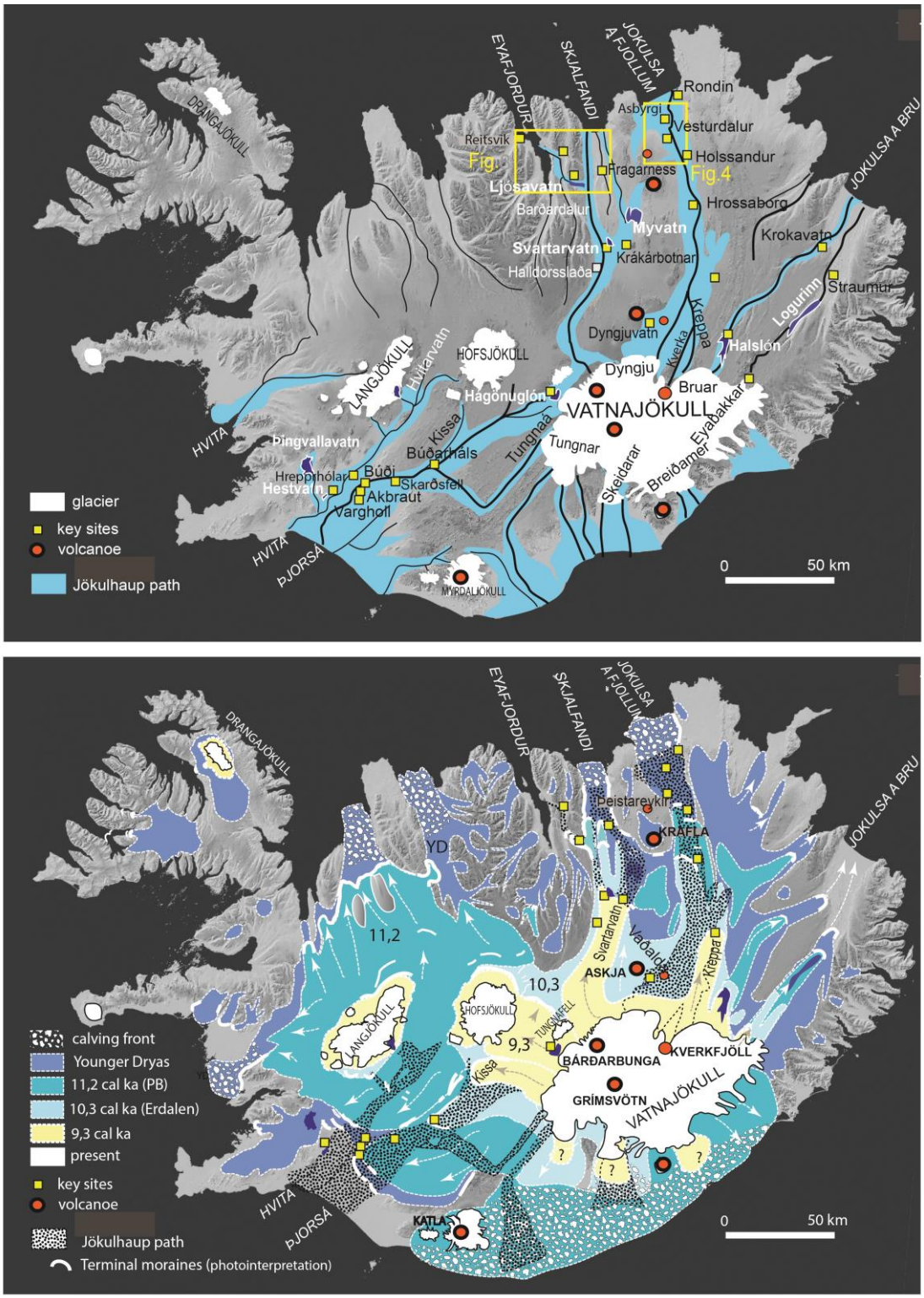

1400

1401 Fig.1

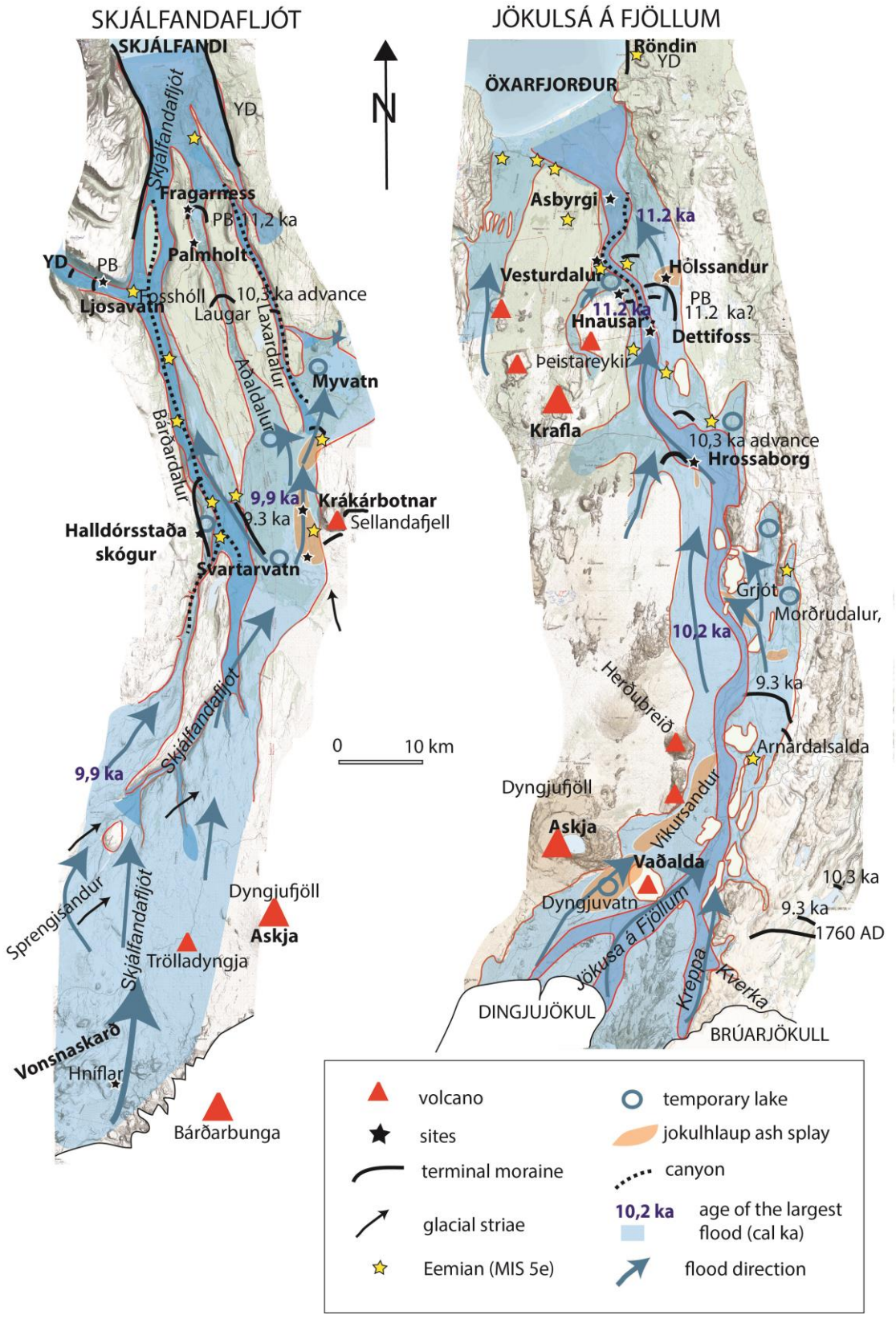

1402

1403 Fig.2

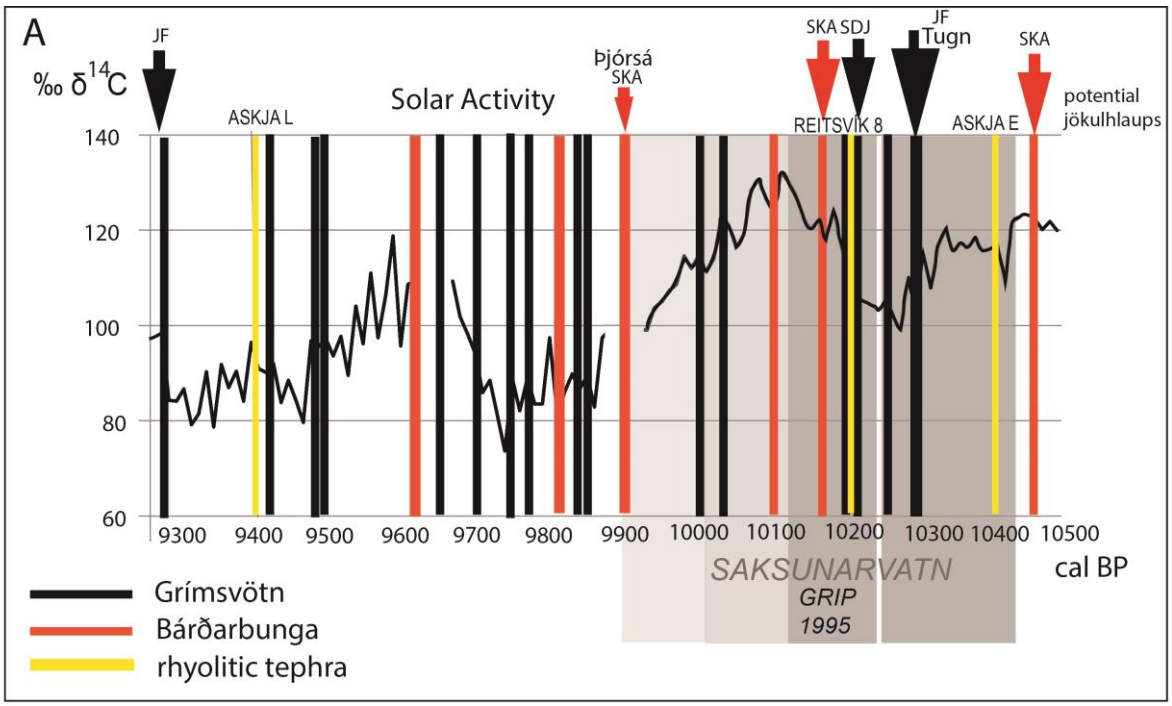

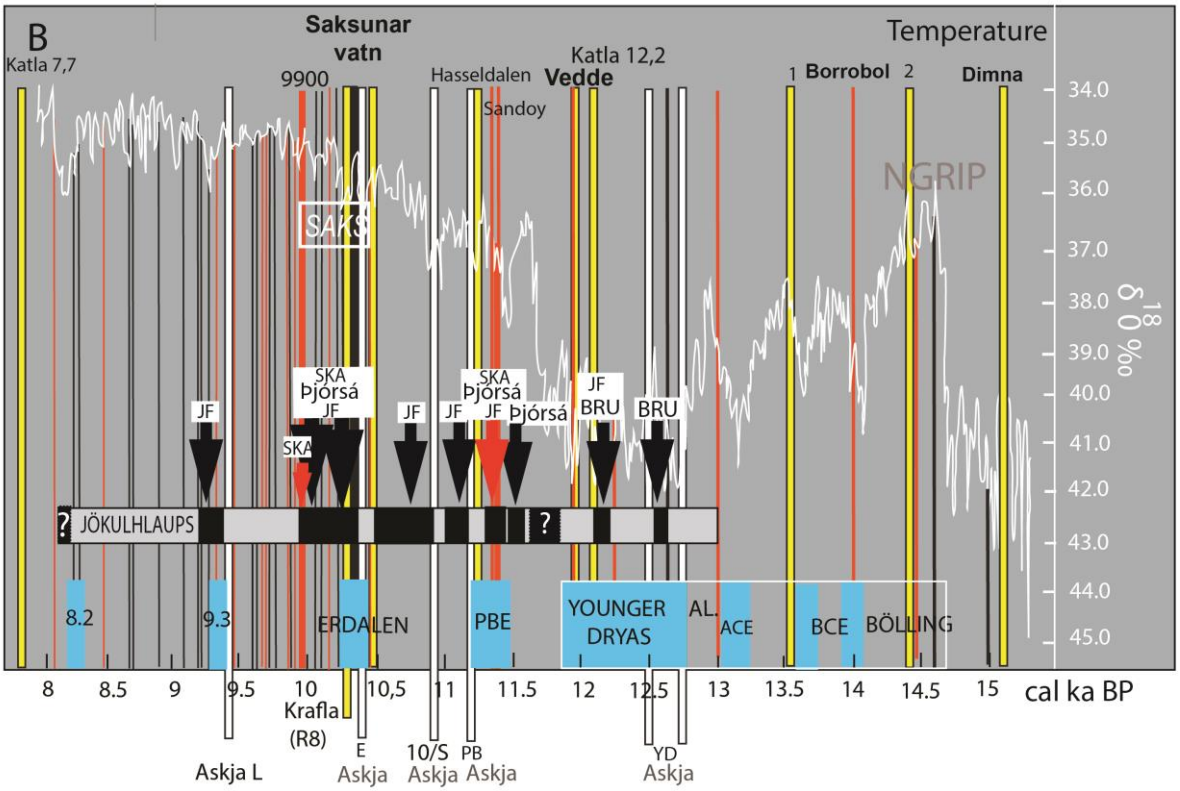

1404

1405 Fig.3

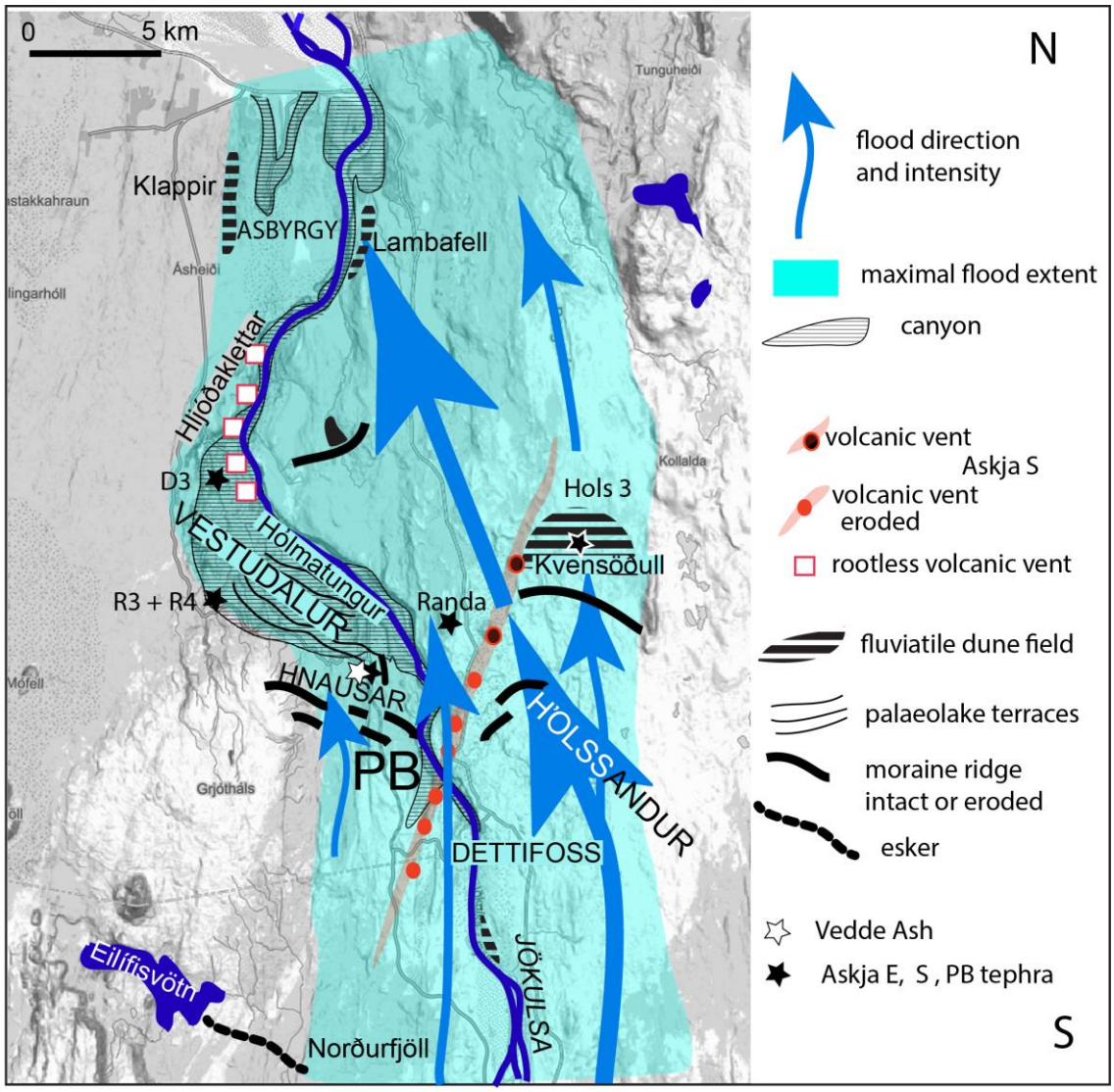

1406

1407 Fig.4

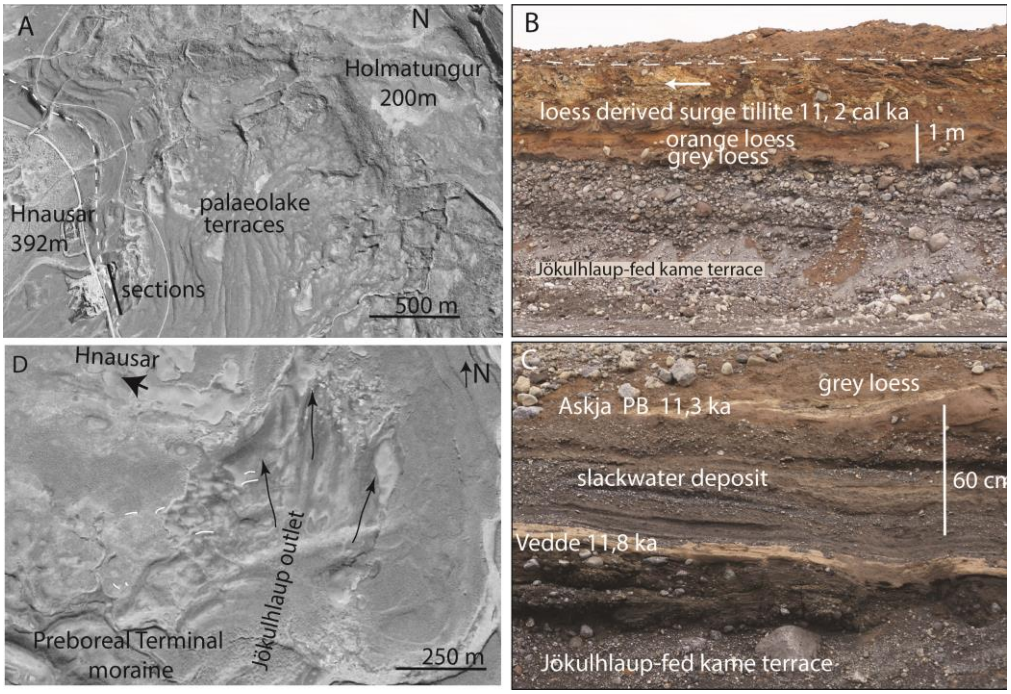

1408

1409 Fig.5

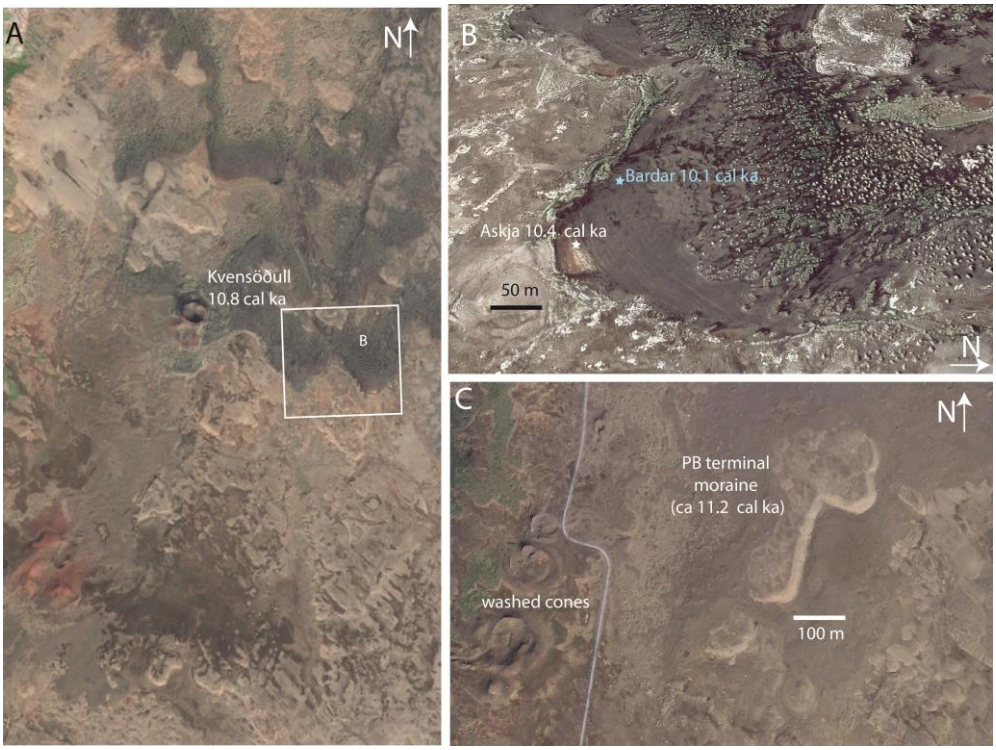

1410

1411 Fig.6

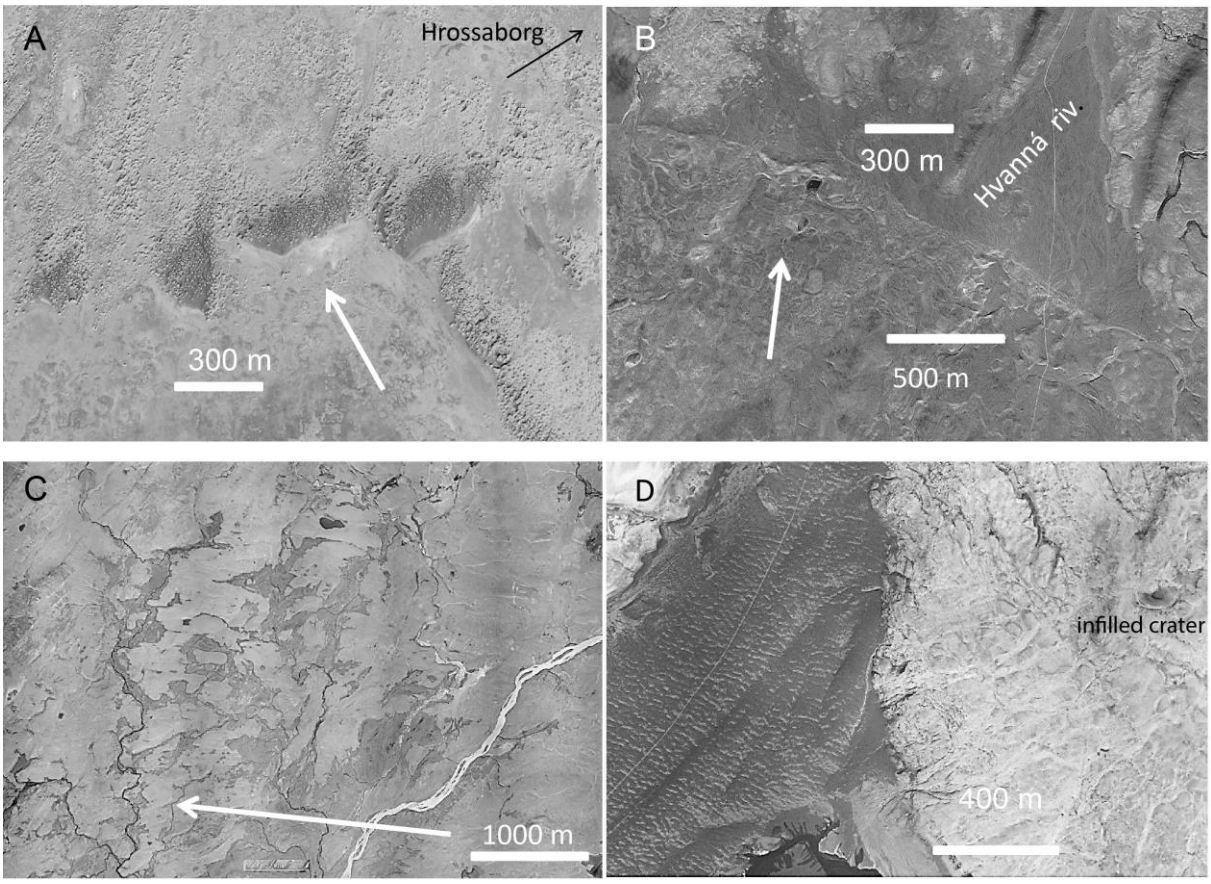

1412

1413 Fig.7

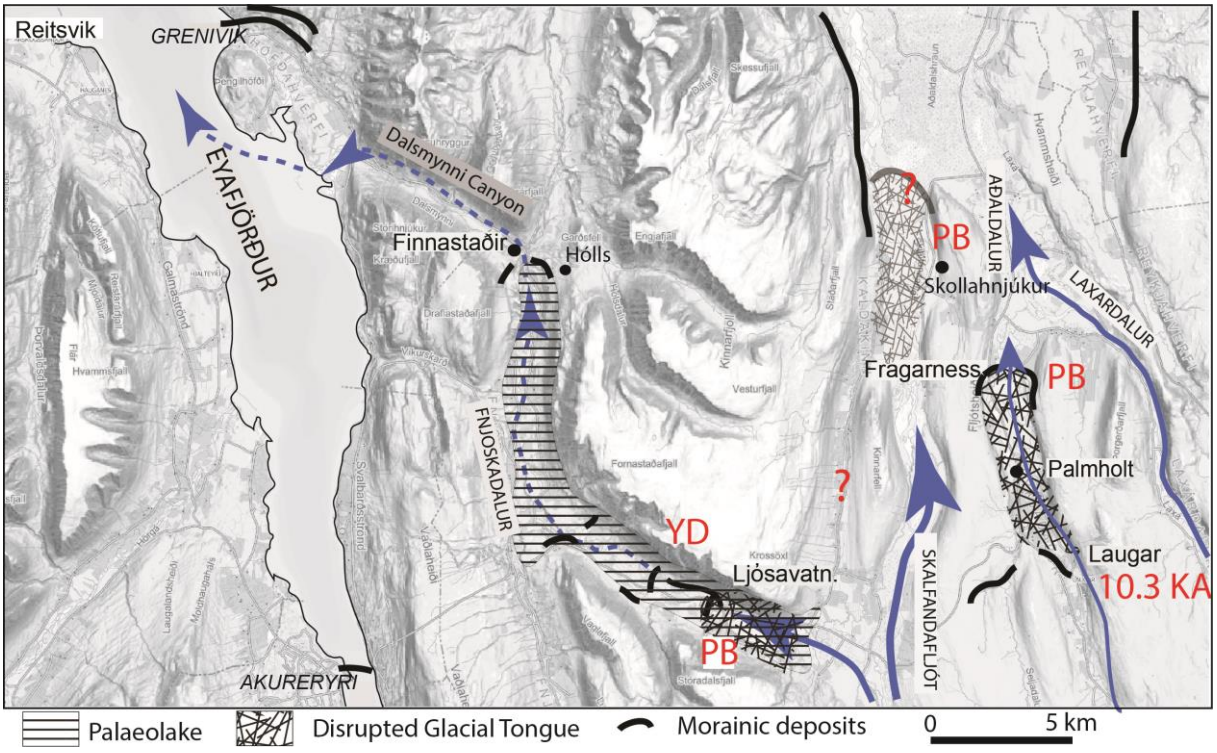

1414

1415 Fig.8

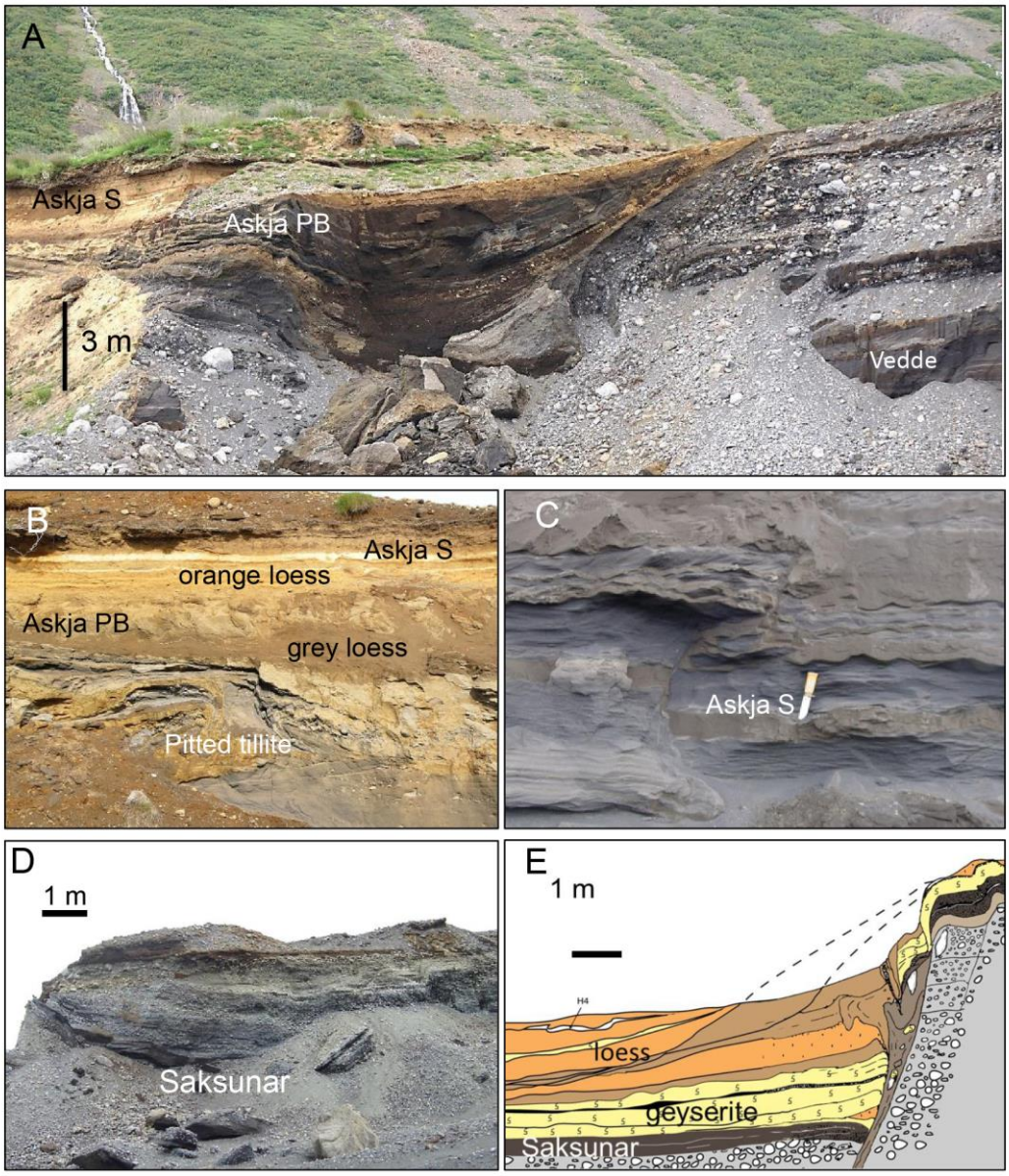

1416
1417 Fig.9

1418

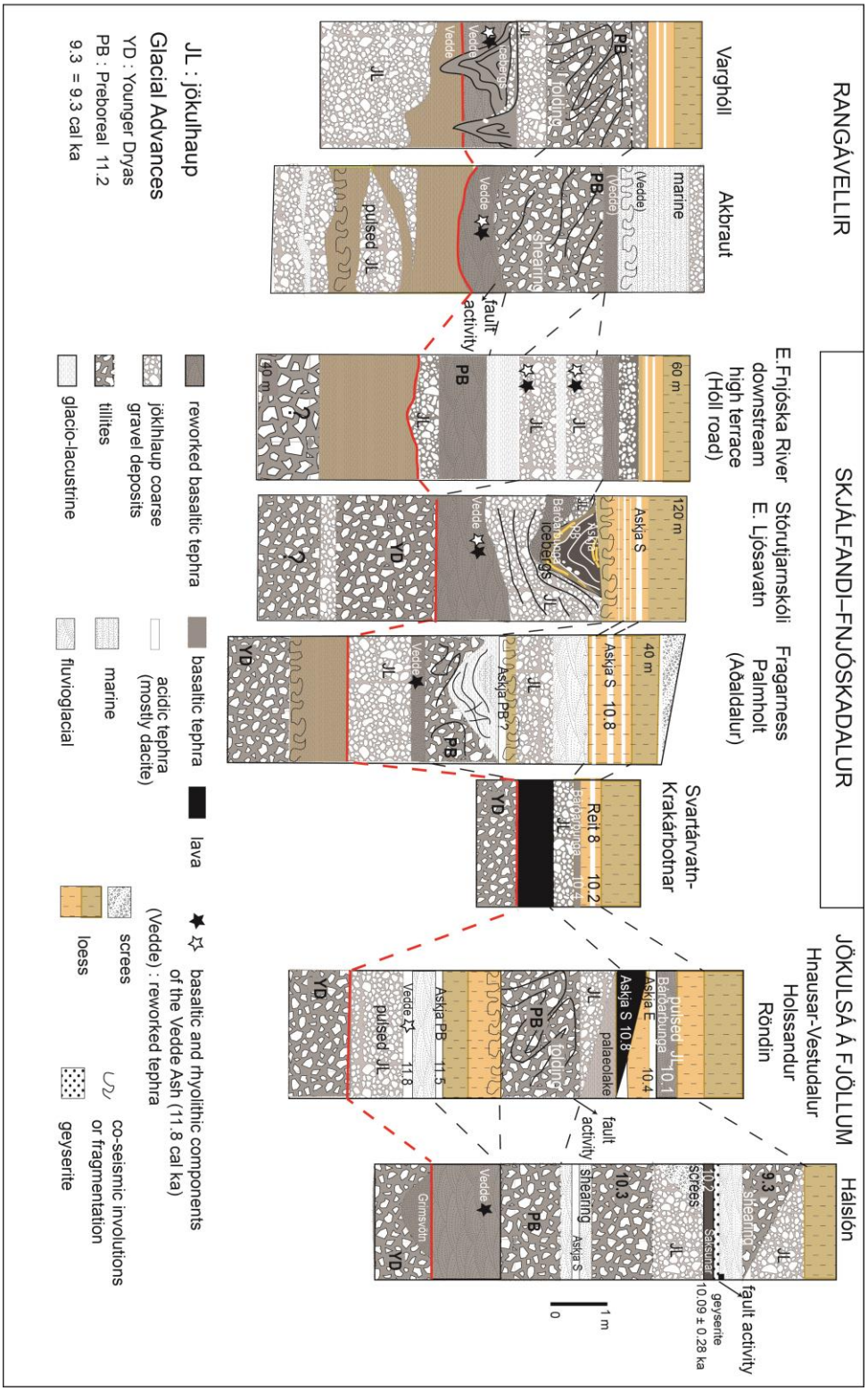

1419

1420 Fig.10

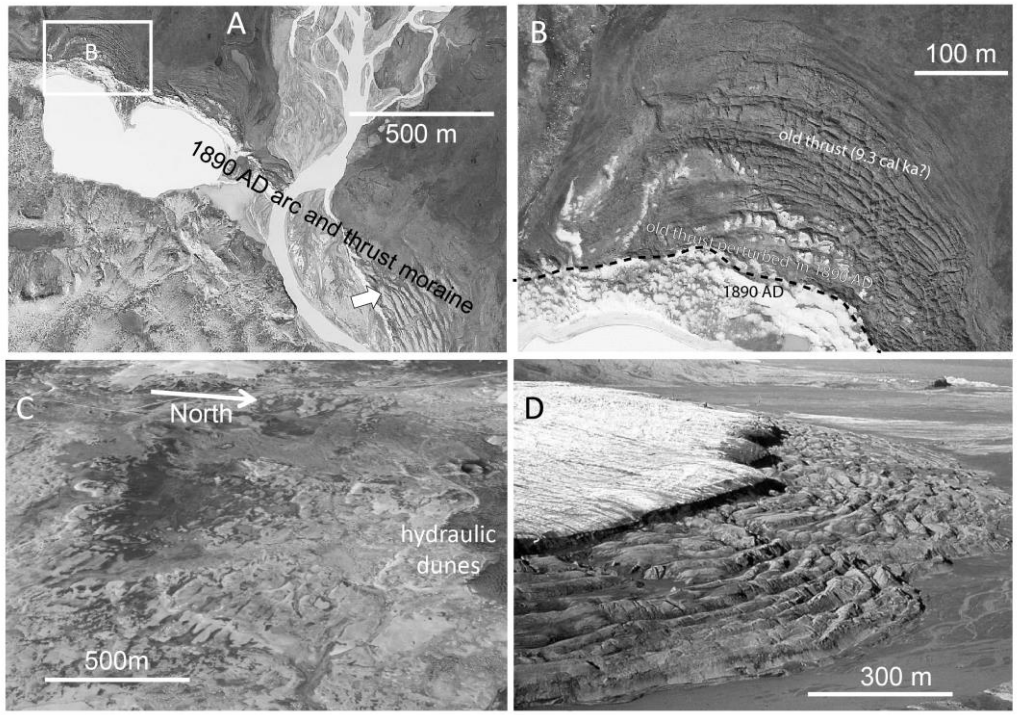

1421

1422 Fig.11

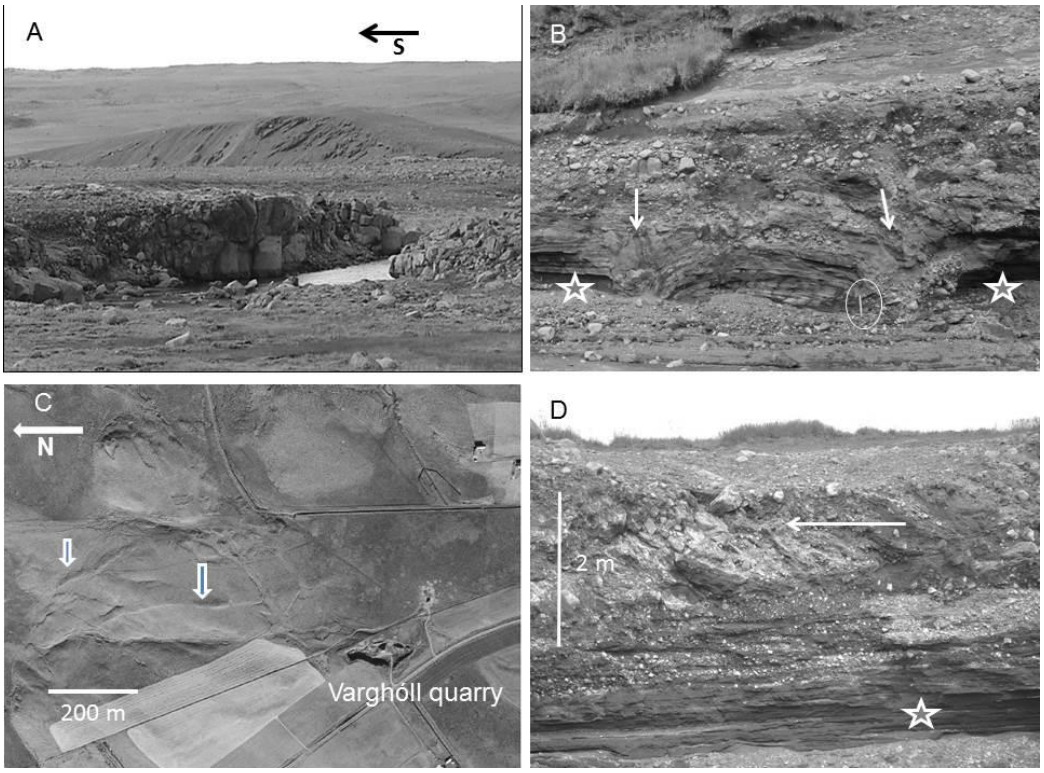

1423

1424 Fig.12

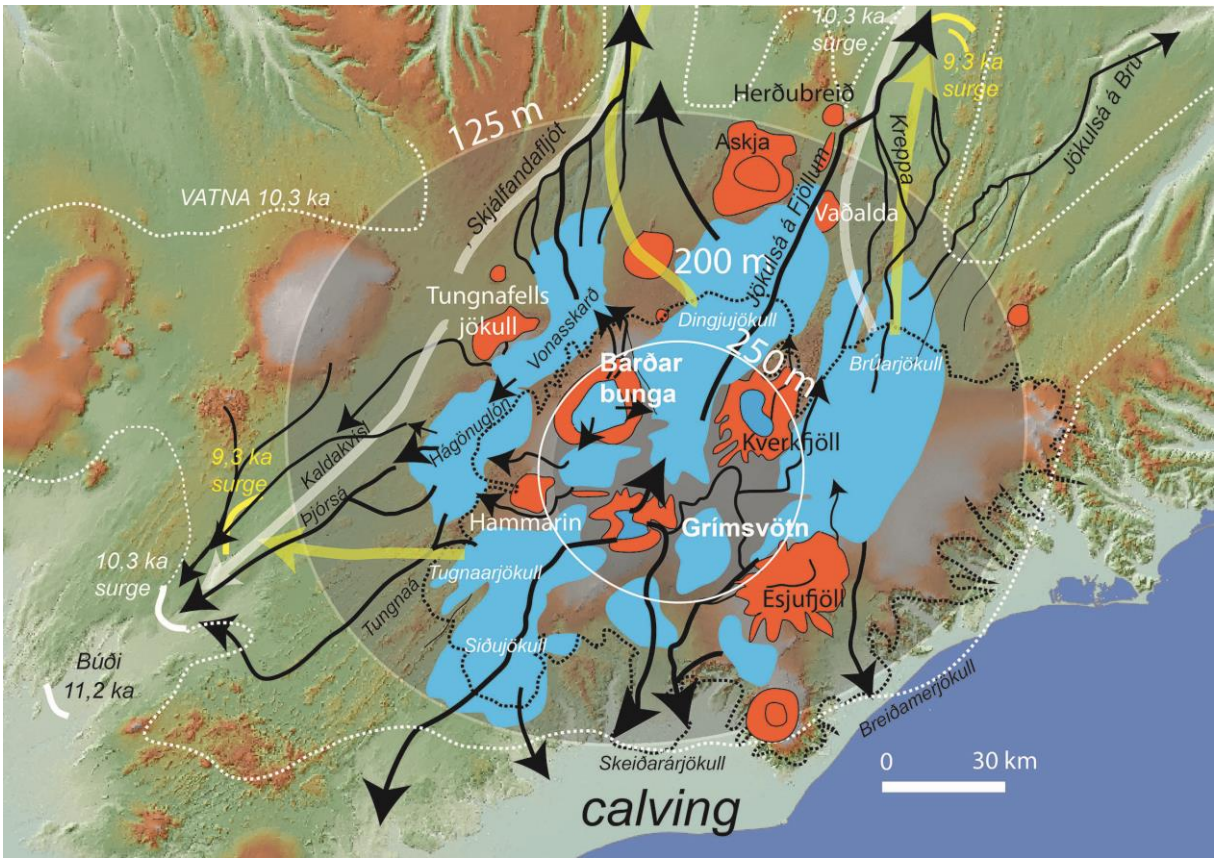

1425

1426 Fig.13